

*Chapter 4*  
***Results and Discussion***

## 4.1. MOLECULAR MODELING ANALYSIS

### 4.1.1. Virtual screening of ERK2 inhibitors *via* hybrid scaffold hopping–FBDD approach

Among the 14 protein structures, after the cross-docking experiment, the ERK2 protein structure with PDB ID: 6GDQ, 1.86 Å (in complex with Ulixertinib) was found to be more suitable for the docking experiment with the lowest average root mean square deviation (RMSD) and thus, selected for *in-silico* study (Table 4.1).

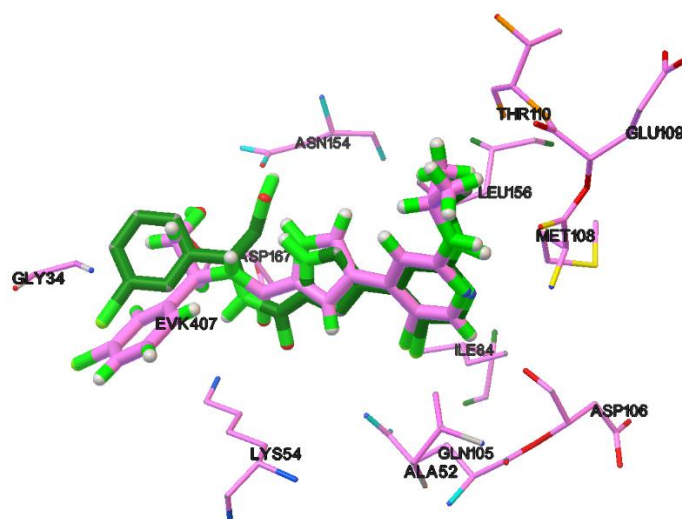
In line with the *in-silico* protocol, Ulixertinib, a clinical trial ERK2 inhibitor, was first subjected to scaffold hopping followed by a series of virtual screening filters including molecular docking and FBDD. Top ten molecules pertaining to novel scaffolds, having optimum similarity score in comparison to Ulixertinib, were selected *via* scaffold hopping using NCI database. Among top ten molecules, Ligand NSC39808 exhibited best shape similarity and feature mapping score of 0.8528 and 0.442, respectively, in comparison to other hits, as given in Table 4.2. It was also observed that all molecules obtained after scaffold hopping retained a carbonyl group and a terminal aryl ring in their structure, quite similar to Ulixertinib. Further, all the identified molecules were validated by molecular docking studies. Special consideration was given to the binding conformation and affinity of the novel scaffolds. The molecules were docked within the catalytic domain of ERK2 protein (PDB ID: 6GDQ). The docking protocol was validated by re-docking Ulixertinib in ERK2. It was observed that the re-docked pose of Ulixertinib occupied the binding pocket in almost similar pose to the co-crystallized Ulixertinib with the RMSD value of less than 1 Å (Figure 4.1).

Table 4.1. RMSD values obtained after cross-docking for the selection of PDB for ERK2.

PDB ID	2OGJ	3SA0	4FV2	6GD Q	4O6E	5BU J	4ZX T	5NH P	5WPI	6G8X	6GJB	6NBS	6RQ 4	6SL G
Ligand														
2OGJ	0.77	8.2	0.89	1.08	1.51	-	0.84	2.42	11.37	0.84	9.09	8.07	7.43	5.34
3SA0	1.02	0.61	5.71	0.52	0.95	-	1.37	0.47	6.91	1.59	3.11	1.87	1.31	2.65
4FV2	0.90	5.79	1.83	0.68	2.31	7.27	0.62	0.79	6.71	0.63	5.99	3.68	3.22	4.31
6GD Q	7.5	7.64	5.60	4.82	5.76	5.37	7.78	6.64	8.13	5.70	9.66	4.36	4.25	4.59
4O6E	4.03	5.29	7.27	5.25	-	2.67	8.74	7.21	-	6.88	9.11	4.59	-	2.35
5BUJ	10.35	9.00	7.71	3.98	6.07	-	7.67	8.25	12.07	7.66	11.49	-	-	-
4ZXT	2.95	2.39	0.83	0.88	1.81	-	0.60	5.66	7.29	3.88	5.89	8.16	0.86	4.16
5NHP	-	-	7.06	-	7.16	-	-	-	7.99	10.72	-	-	1.45	-
5WPI	10.49	-	11.48	10.7	10.99	-	11.86	13.27	1.92	15.19	15.91	-	-	5.83
6G8X	0.89	0.83	0.96	0.94	1.40	-	0.96	0.86	7.82	0.61	7.35	5.25	1.63	1.68
6GJB	5.70	8.26	3.47	4.49	4.07	-	5.84	5.85	6.01	5.90	0.26	0.85	8.52	2.43
6NBS	2.24	1.38	4.46	1.42	1.33	-	1.37	6.28	4.51	2.38	3.48	0.74	6.32	1.11
6RQ4	3.59	6.03	1.65	2.19	1.89	-	3.41	4.12	0.88	1.67	2.17	4.35	1.23	4.37
6SLG	1.05	2.11	1.71	0.91	1.56	-	2.73	7.94	5.36	4.39	1.35	6.26	4.12	0.52
Average	3.67	4.10	4.33	2.70	3.34	-	3.83	4.98	6.21	4.86	6.01	3.44	3.36	3.27

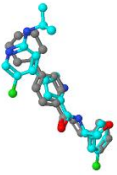
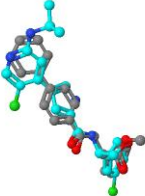
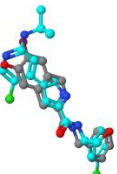
\* Average RMSD value showed best fitting for PDB ID: 6GDQ, which is selected for further study.

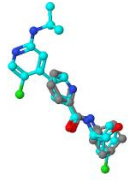
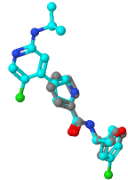
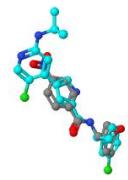

Docking results (Table 4.3.) revealed that all the ligands fit into the binding pocket of ERK2 (Figure 4.2A) but only Ligand NSC39808 completely occupied the binding pocket while other hits (Figure 4.2B), due to their flexibility, folded in to the hinge region and did not occupy well the binding pocket (Figure 4.2C). This property of restricted flexibility which led to an improved binding of the scaffold formed the basis of its selection. Additionally, NSC39808 showed good binding energy score (-7.77 kcal/mol), closer to binding energy score of Ulixertinib (-8.39 kcal/mol). Thus, docking analysis proved NSC39808 as good scaffold which possesses similar binding properties as Ulixertinib.

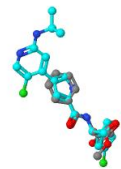
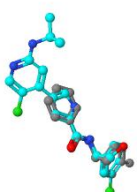
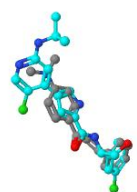


**Figure 4.1.** 3D conformation of re-docked Ulixertinib (green) in the binding pocket of ERK2 with co-crystallized bioactive conformation of Ulixertinib (pink).

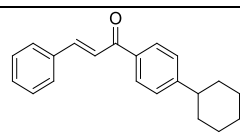
**Table 4.2.** Top ranked superimposed compounds identified by scaffold hopping.

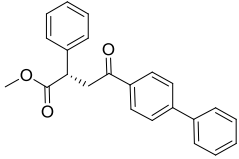
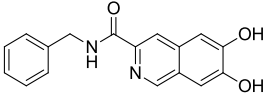
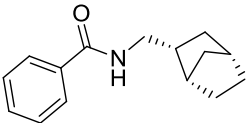
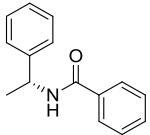
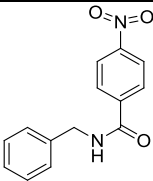
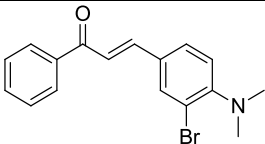
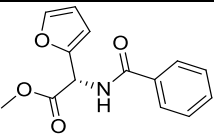
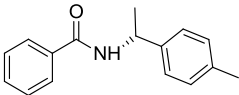
Rank	Ligand ID	Structure	Score	Shape similarity score	Feature mapping score
1	NSC39808		1.295	0.8528	0.442
2	NSC2402		1.278	0.8473	0.4312
3	NSC666245		1.278	0.8131	0.4653

4	NSC167463		1.273	0.7079	0.5656
5	NSC100227		1.272	0.7593	0.5131
6	NSC405529		1.255	0.7698	0.4852
7	NSC643164		1.253	0.716	0.5371

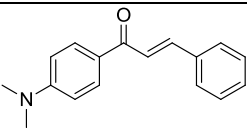
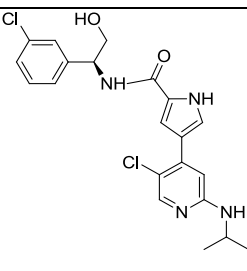
8	NSC655423		1.244	0.726	0.5185
9	NSC251017		1.242	0.751	0.4909
10	NSC49901		1.24	0.7766	0.4634

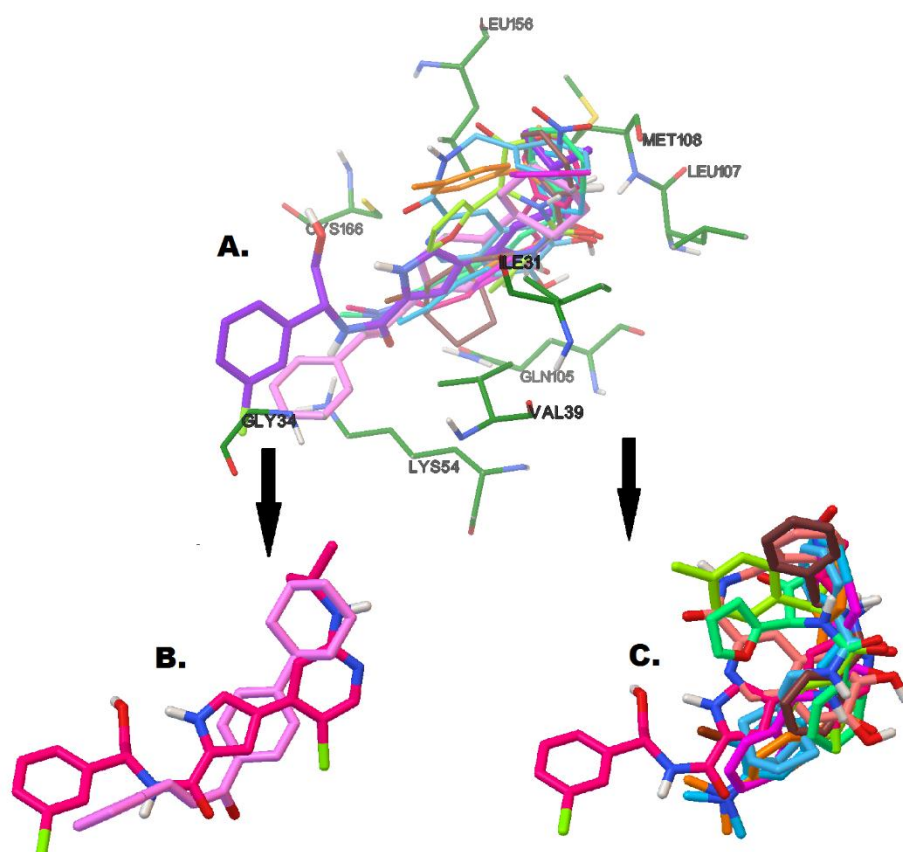
**Table 4.3.** Results obtained after validating the hits obtained from scaffold hopping *via* docking analysis.

Ligand ID	Structure	Binding energy (kcal/mol)	H-bond	Predicted activity
NSC39808		-7.77	Met108	2.01 $\mu$ M

NSC2402		-7.25	Met108	4.88 $\mu\text{M}$
NSC666245		-7.12	Met108	6.05 $\mu\text{M}$
NSC167463		-7.03	Met108	7.02 $\mu\text{M}$
NSC100227		-6.9	Met108	8.68 $\mu\text{M}$
NSC405529		-7.53	Gln105	3.03 $\mu\text{M}$
NSC643164		-7.74	Met108	2.11 $\mu\text{M}$
NSC655423		-5.62	Met108	76.12 $\mu\text{M}$
NSC251017		-6.44	Met108	19.09 $\mu\text{M}$



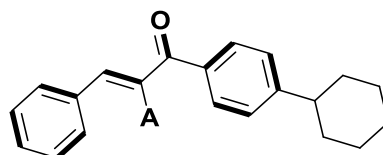
NSC49901		-7.14	-	5.84 $\mu$ M
Ulixertinib		-8.39	Met108	0.76 $\mu$ M



**Figure 4.2.** A) Overlapped representation of the identified novel scaffolds in the catalytic domain of ERK2 (NSC39808: light pink; NSC2402: peach; NSC666245: sky blue; NSC167463: Brown; NSC100227: dark pink; NSC405529: blue; NSC643164:

fluorescent green; NSC655423: green; NSC251017: yellow; NSC49901: pink; Ulixertinib: Purple). **B)** 3D conformation of the selected scaffold (**NSC39808**; light pink) along with active conformation of Ulixertinib (dark pink). **C)** Rest of the identified hits after scaffold hopping, along with Ulixertinib (dark pink).

Following the selection of **NSC39808** as the top hit with novel scaffold, *i.e.* chalcone, it was subjected to FBDD for discovery of new hits with varied substitutions (fragments) and increased binding affinity and potency for ERK1/2. A fragment deconstruction and fragment linking approach was used to perform the study. Para-Gen module of ACIFS server assigned the total formal charge using auto-calculate, charge method was specified as gas, and no cofactor was considered in the binding site. Core-gen module identified the core framework of the ligand and resulted in various cores in response to our selected hit, **NSC39808**. For the current study, chalcone framework was selected as “core” to perform fragment linking, as shown in **Figure 4.3**. and this core was subjected for Cand-gen module to screen the FDA approved fragment library for FBDD search (Hao, Jiang et al. 2016).

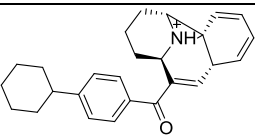
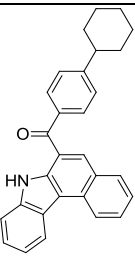
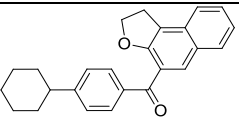


**Figure 4.3.** Core selected to submit to CAND-GEN module for FBDD search.

The Cand-gen resulted in hits with excellent binding energy (MM-PBSA score) as given in **Table 4.4**. To validate these results, top 10 hits were selected and were subjected to molecular docking analysis, which concluded that all 10 molecules demonstrated good binding energy score (Autodock docking score), even better than standard Ulixertinib (**Table 4.5**). The overlapped 3D protein-ligand interaction diagram of the top 10 screened hits for supposed ERK2 inhibitory potential is shown in **Figure 4.4A**. Among all, three hits, Ligand **6**, **8** and **10**, preserved the required essential H-bond interaction with Met108, parallel to that of Ulixertinib, which is

established as an essential prerequisite for ERK2 inhibitory potential (Samatar 2017; Pathania and Rawal 2020). Besides, ligand **10** exhibited top binding energy amongst these top three hits (-8.59 kcal/mol), even better than Ulixertinib (-8.39 kcal/mol). Interestingly, Ligand **1** and **2** did possess higher binding affinity than other hits (more than -9.0 Kcal/mol) in the molecular docking analysis but they did not maintain H-bond interaction with Met108 and thereby are suspected to be “false-positives”. While Ligand **6** and **8** did maintain the key interactions as well as possessed decent binding affinity and thus, along with Ligand **10**, can be considered potent putative ERK2 inhibitor (**Figure 4.4B**).

**Table 4.4.** Top ten compounds identified from FBDD analysis.

Ligand ID	Structure & Binding mode	$\Delta H(\text{PB})$ (kcal/mol)	$\Delta H(\text{GB})$ (kcal/mol)	-TAS (kcal/mol)	$\Delta G(\text{PB})$ (kcal/mol)	$\Delta G(\text{GB})$ (kcal/mol)
1		-37.500	-30.270	22.340	-15.160	-7.930
2		-18.260	-30.310	18.721	0.461	-11.589
3		-15.260	-30.260	17.715	2.455	-12.545

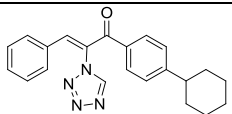
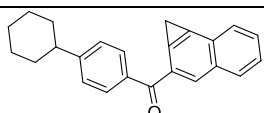
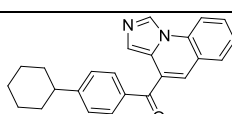
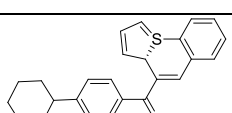
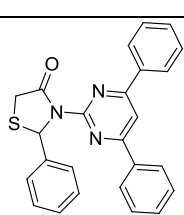
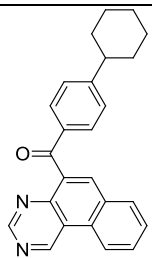
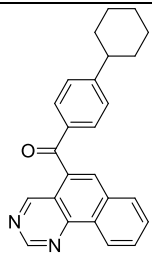
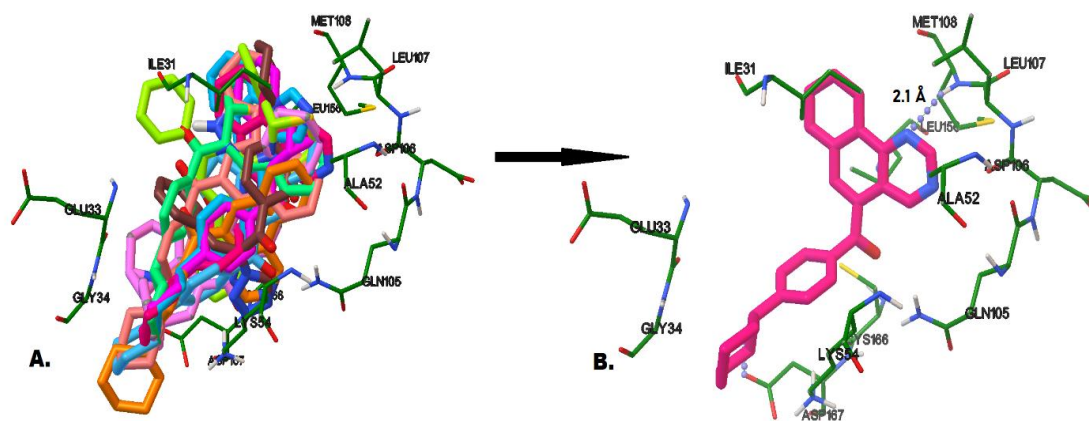
4		-12.480	-30.390	15.468	2.988	-14.922
5		-12.570	-30.220	16.512	3.942	-13.708
6		-9.030	-30.220	13.542	4.512	-16.678
7		-12.140	-30.420	16.864	4.724	-13.556
8		-10.360	-30.240	16.020	4.755	-13.140
9		-8.680	-30.260	17.564	8.884	-12.696
10		-8.300	-30.310	16.615	8.315	-13.695

Table 4.5. Docking score of hits obtained from CAND-GEN.

Ligand ID	Binding energy (kcal/mol)	H-bond	Predicted activity
1	-9.31	LYS54	0.14 $\mu$ M
2	-9.65	-	0.08 $\mu$ M
3	-8.31	GLN105	0.81 $\mu$ M
4	-9.45	ASP167	0.11 $\mu$ M
5	-8.53	-	0.56 $\mu$ M
6	-8.46	MET108	0.63 $\mu$ M
7	-9.24	-	0.16 $\mu$ M
8	-8.41	MET108	0.68 $\mu$ M
9	-8.71	ASP167	0.41 $\mu$ M
10	-8.59	MET108	0.51 $\mu$ M
Ulixertinib	-8.39	MET108	0.76 $\mu$ M



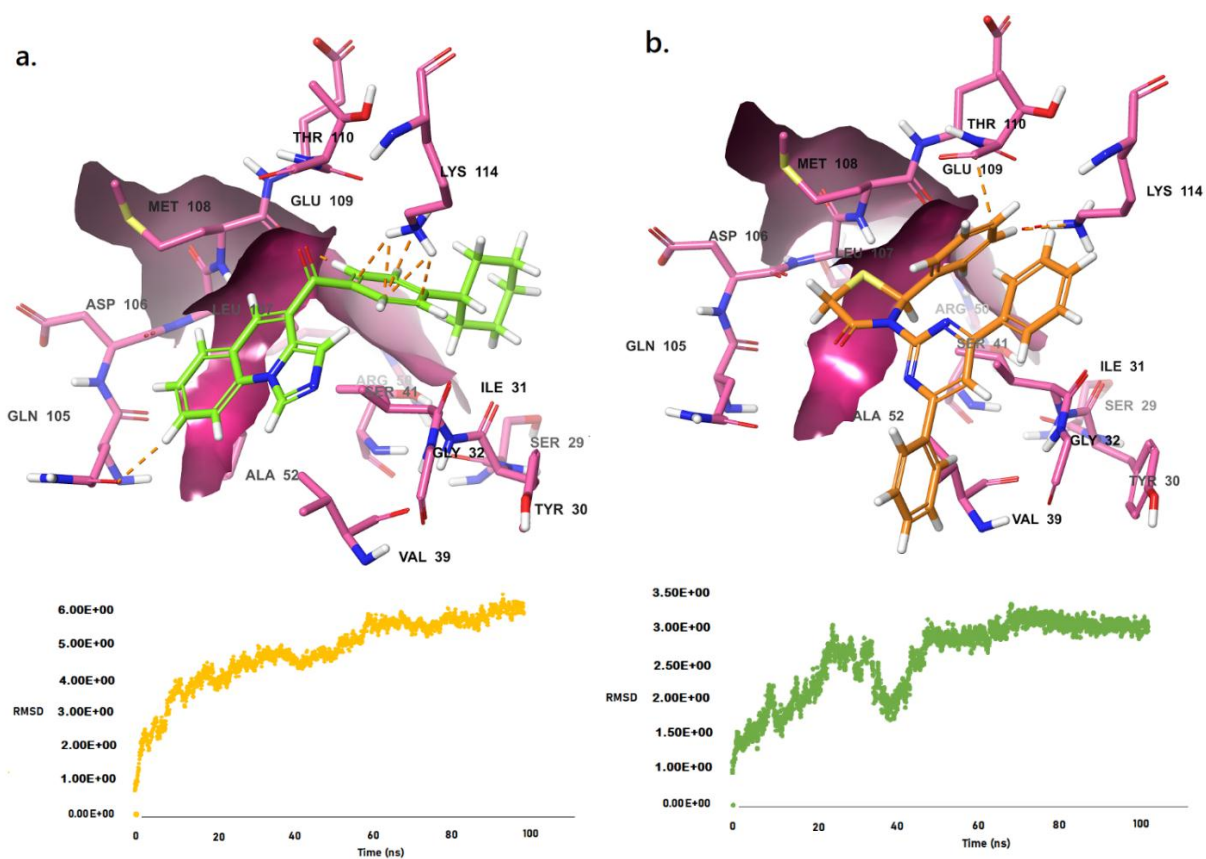
**Figure 4.4.** A) Overlapped 3D interaction diagram of the top 10 identified novel hits for putative ERK2 inhibitory potential. B) 3D interaction diagram of best hit (Ligand 10) in the catalytic domain of ERK2.

In the last step, a molecular dynamic simulation was performed to validate the obtained results. It was run to analyze and validate the binding orientation, stability of the complex and binding affinity of the selected hits within the binding pocket of ERK2. Therefore, the docked complexes of 3 top hits screened as alleged inhibitors with ERK2 were forwarded for the MD simulation experiments. Overall, these ligand-protein complexes were forwarded to MD simulations analysis with the production run of 100 ns. Critical evaluation of 3D ligand-protein interaction diagrams showed that the top molecule, Ligand 10 maintained the key interactions in the catalytic domain of target protein, which are reported mandatory for inhibitory potential, thus, justify the assertion of probable inhibitors. More importantly, the essential H-bond interaction between Ligand 10 and Met108 was retained over the simulation time period. Moreover, complexes were analyzed to determine their stability by calculating and analyzing the RMSD plot of the top hits with the protein backbone, as shown in **Figure 4.5**. The values were found in the range of 2.0–2.5 Å for Ligand 10. While for ligand 6 and ligand 8, the values were found to be in the range of 5.0-6.0 Å and 2.5-3.0 Å, respectively. The variations in initial run of MD, shown via RMSD, can be explained by slight adjustments which occur in the beginning of a simulation run. However, overall RMSD plot and binding interactions within the binding cavity of the target protein establish that complexes were stable after the simulation run. Also, the top hits retained key interactions with the catalytic domain amino acid residues including Met108, Lys114, Leu107, Lys54, Gly34, Asp106, Ser 153, Ala52, Gly32 and Ile31 of ERK2, after the complete simulation run, suggesting putative inhibitory potential of the screened hits. Further, the energy liberated during a ligand-protein interaction is determined more accurately via calculation of binding energy. The final binding energy is a sum of polar solvation, van der Waals, electrostatic, and SASA energy. MM-GBSA method was employed to determine the relative affinity of the best hits with ERK2 protein. Results showed the binding energy value of -21.92 kcal/mol for the top hit (ligand 10) within the catalytic domain of ERK2. Similarly, Ligand 6 and 8 also showed good binding energy values of -27.89 kcal/mol and -

32.22 kcal/mol, respectively (**Table 4.6.**). Further we analyzed the contribution of key residues in the binding energy by reviewing the decomposition data. Residues such as Leu 107, Met108 and Lys114 contributed favorably in the formation of the complex. In the free protein, these cavity residues, Leu107, Met108 and Lys114 contributed -34.05, -38.64 and -48.46 kcal/mol energy, respectively, in the overall binding energy while upon complex formation with the Ligand **10**, the energy contribution varied favorably to -37.79, -42.30 and -49.12 kcal/mol.

**Table 4.6.** Various component of the MM-GBSA binding score for Ligand **6**, **8** and **10**.

S. No.	Energy components	Ligand 6 (kcal/mol)	Ligand 8 (kcal/mol)	Ligand 10 (kcal/mol)
1.	MM-GBSA dG Bind vdW	-44.24	-49.48	-35.13
2.	MM-GBSA dG Bind Solv GB	20.04	32.74	33.69
3.	MM-GBSA dG Bind SelfCont	0	0	0
4.	MM-GBSA dG Bind Packing	-0.08	-0.49	0
5.	MM-GBSA dG Bind Lipo	-18.10	-18.81	-16.51
6.	MM-GBSA dG Bind Hbond	-0.33	-0.99	-8.78
7.	MM-GBSA dG Bind Covalent	14.74	12.35	12.6
8.	MM-GBSA dG Bind Coulomb	0.07	-7.52	-7.79
<b>9.</b>	<b>Overall MM-GBSA dG Bind</b>	<b>-27.89</b>	<b>-32.22</b>	<b>-21.92</b>





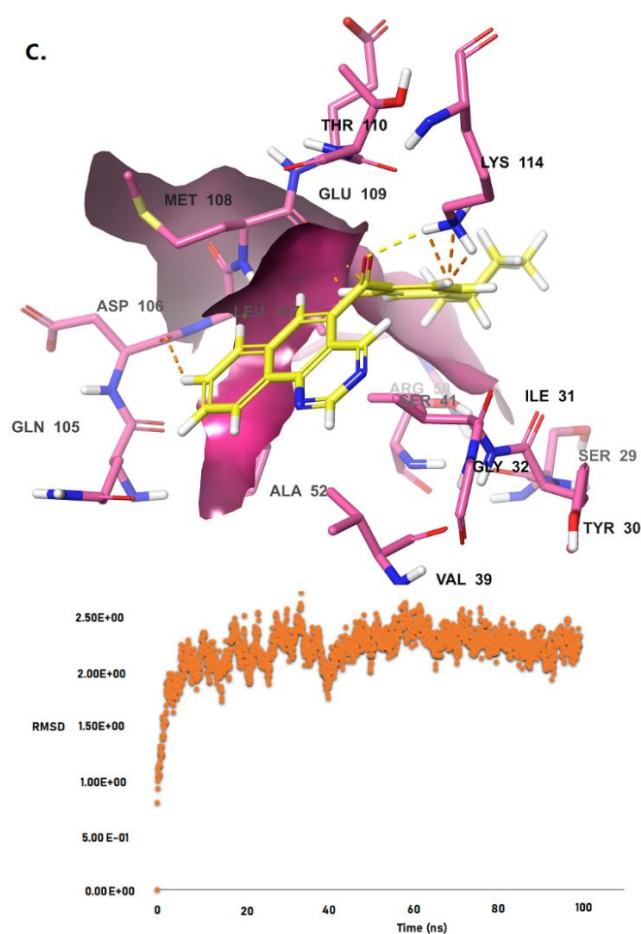


**Figure 4.5.** 3D interaction diagram of best hits: (a) Ligand 6; (b) Ligand 8; (c) Ligand 10; in the catalytic domain of ERK2, along with the RMSD plot.

Frontier orbital theory underlines those shapes and symmetries of HOMO and LUMO orbitals play crucial role in the stability of a molecule in the ligand-receptor interactions. In a HOMO-LUMO map, blue color specifies positive lobes while red color describes negative lobes. The effect of HOMO energy directly regulates the charge transfer during  $\pi$ - $\pi$ , or  $\pi$ - $\sigma$  stackings between aromatic rings of the ligands and the amino acid residues, thereby regulating the binding affinity. The HOMO and LUMO energy values were computed and the energy difference (band energy gap)  $\Delta E$  (LUMO-HOMO) was then derived to understand the reactivity at molecular level. A low band energy gap is predictive of a reactive compound while a wide energy gap

implies that the activity is not sufficient at the active site of a protein receptor (Queiroz, Gomes et al. 2009). The 2D representation of top hits has been displayed in **Figure 4.6**. Ligand **6** showed the least band energy gap of 0.136 and thus was strongly supported to have a strong inhibitory activity in the binding domain of ERK2. DFT analysis showed that Ligand **6** also displayed highest HOMO energy (-0.200 eV), indicating its good affinity for ERK2. While as per the maximum hardness principle, a slightly larger energy gap for Ligand **8** ( $\Delta E$  of 0.146) and 10 ( $\Delta E$  of 0.150) indicates slightly lower activity. As final step of the *in-silico* protocol, prediction of the pharmacokinetic parameters was performed for the top hits, as given in **Table 4.7.**, using a web-server for systematic ADMET evaluation, ADMETlab (Dong, Wang et al. 2018).

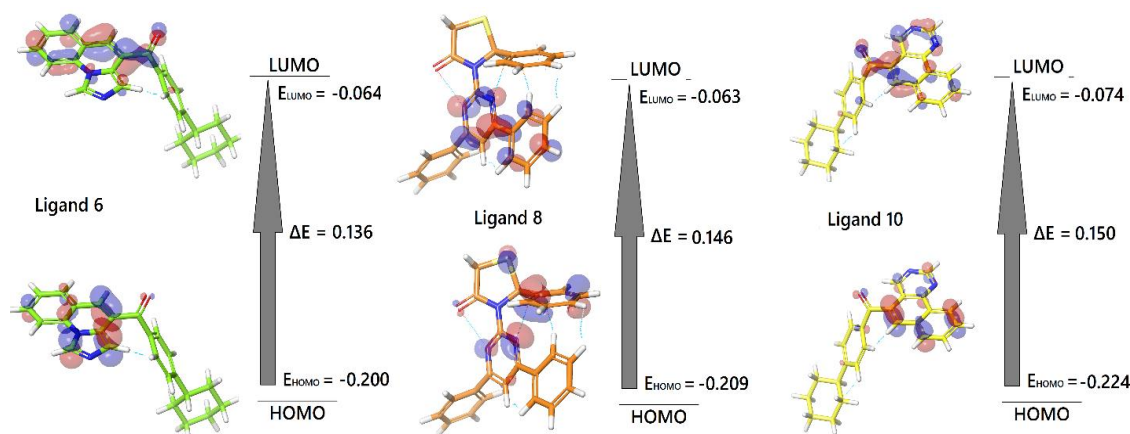


**Figure 4.6.** The orbital energy values and energy gap for Ligand **6**, **8** and **10**.

**Table 4.7.** Various pharmacokinetic parameters predicted for the Ligand **6**, **8** and **10**.

Compound	logS	logD	logP	caco2	VD	PPB	CL	T	Pgp	HIA
<b>Ligand 6</b>	-6.33	3.248	5.766	-4.68	0.56	81.38	1.613	2.378	0.022	0.872
<b>Ligand 8</b>	-6.09	3.217	5.589	-4.73	0.016	82.67	1.202	2.209	0.025	0.821
<b>Ligand 10</b>	-6.33	3.345	6.062	-4.76	0.305	82.70	1.294	2.222	0.012	0.877

\* VD; volume of distribution, PPB; plasma protein binding, CL; clearance, T; half-life, Pgp; probability of Pgp substrate, HIA; probability of human intestinal absorption

### 4.1.2. Improving binding affinity of the virtually screened hit (Ligand 8) via optimizing substituents (Formula-I)

After obtaining three hits (Ligand 6, 8 and 10) we focused on optimizing one of the hits identified in the *in-silico* study for the development of potent ERK2 inhibitors. Novel hit (Ligand 8) obtained from the *in-silico* results which forms crucial interactions in the binding domain of ERK2 was selected because of its simple chemistry. Due to the hydrophobic nature of the pocket, for the inhibitors mimicking Type-II binding mode, the binding affinity is dependent on both the overall hydrophobic packing of the ligand and conserved hydrogen bond interactions with key amino acid residues such as Lys54 and Met108 in the ATP-binding domain. Therefore, a library of around 100 derivatives of thiazolidinone-pyrimidine (Ligand 8) derivatives was prepared by incorporating diverse hydrophobic substituents at different sites on the core structure (**Figure 4.7.**) and subjected to *in silico* evaluation to filter out derivatives with improved binding affinity for ERK2, in comparison to reference (Ligand 8), followed by their synthesis, characterization and evaluation of their *in-vitro* potential as ERK2 inhibitors

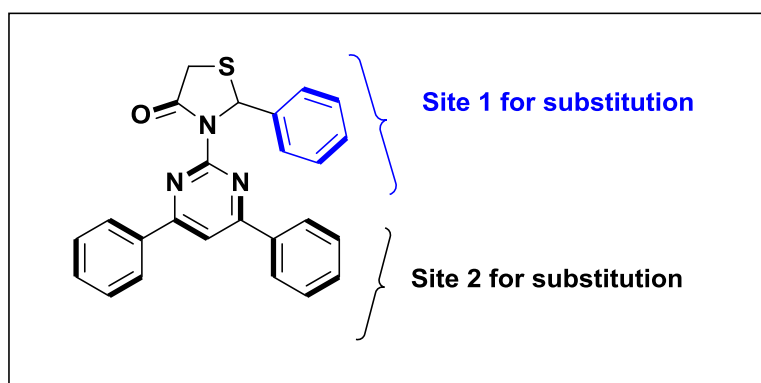


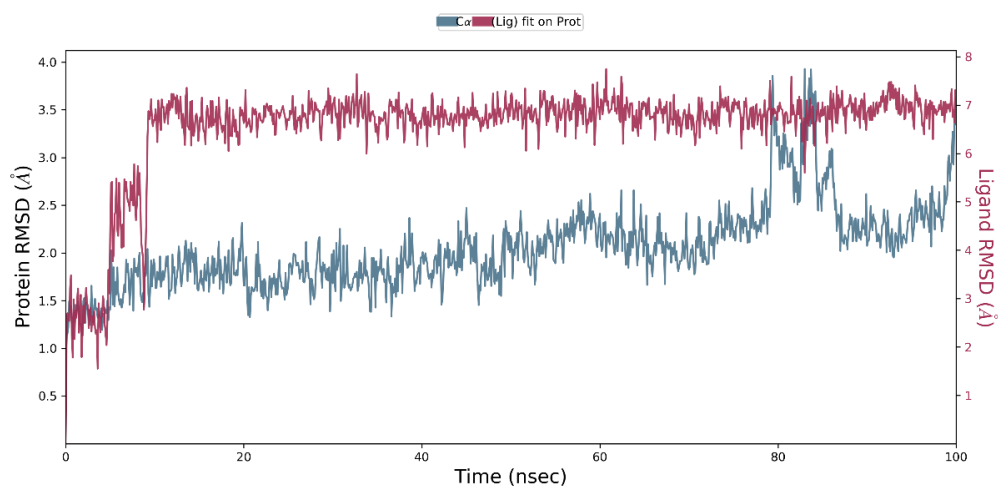
**Figure 4.7.** Different sites on the core structure of Ligand 8 explored to generate an *in-house* library.

A library of thiazolidinone-pyrimidine (Ligand 8) derivatives was prepared, energy minimized and subjected to *in-silico* analysis. Both thiazolidinone and pyrimidine-based compounds are well known for potent pharmacological profile (Rawal,

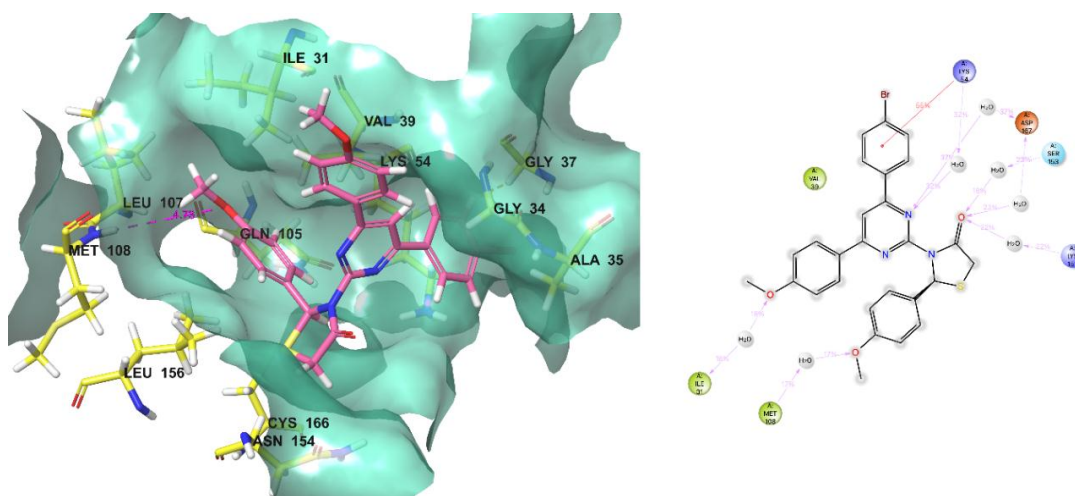
Prabhakar et al. 2005; Rawal, Tripathi et al. 2007; Rawal, Tripathi et al. 2008). Various analogues of the selected lead (Ligand **8**) were docked in the co-crystallized protein structure of ERK2. Derivatives maintaining the essential conserved interactions in the binding pocket of ERK2, such as H-bond interactions with Met108 were screened and selected for further analysis involving MD simulations for 100 ns and binding affinity analysis. The designed molecules which retained this key interaction and maintained a stable complex with the ERK2 were then forwarded for the determination of binding affinity (MM-GBSA score).

Out of all derivatives present in the library, a total 15 molecules were found to possess equal or more than equal docking scores (glide scores) in comparison to the lead (Ligand **8**), ranging from 6.57-4.54 kcal/mol, within the catalytic domain of ERK2 (Table 4.8.). After the MD simulation of 100 ns, the RMSD values were determined to study the stability of the complexes. The RMSD plot of the designed compounds in complex along with native protein backbone atoms revealed complexes to be fairly stable. The graph for the same (**8j**), plotted against time, is shown in Figure 4.8. Importantly, a deviation of around 1.5 Å is observed between 79th ns and 85th ns of the simulation run. However, the complex regains its stability afterwards and stays stable for remaining time period (15 ns) of the simulation run. To assess the impact of this deviation on the ligand-protein interactions, snapshot of the complex at each 10 ns was studied. Upon establishing the stability of the complexes, interaction plot of the designed molecules in the binding pocket of ERK2 were studied to generalize their binding mode. It revealed that the carbonyl functionality in the thiazolidinone acts as H-bond acceptor and connects through a theoretical water bridge with Lys151, Ser153 and Asp167. Additionally, in case of some of the selected compounds, pyrimidine nucleus acts as H-bond acceptor for crucial amino acid residue Lys54. While, in some of the designed molecules, -OCH<sub>3</sub> on the aryl ring substituted on the thiazolidinone nucleus interacted with the hinge region amino acid residues including Met108 *via* theoretical water bridge. Importantly, the top hits retained key interactions network in the binding pocket of ERK2 which involved catalytic domain amino acid

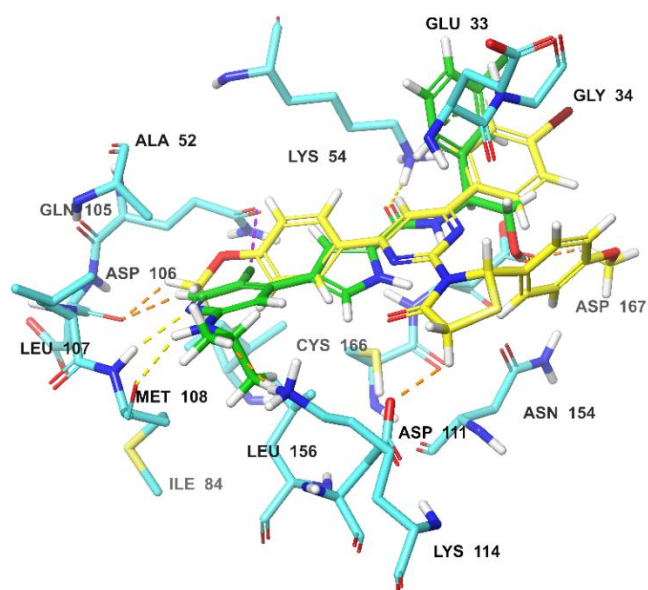
residues such as Met108, Lys114, Leu107, Lys54, Gly34, Asp106, Ser 153, Ala35, Gly37, Ile56 of ERK2, after the complete simulation run, suggesting putative inhibitory potential of the screened hits. 3D interaction diagram for one of the selected molecules (**8j**) in the binding pocket of ERK2 is shown in **Figure 4.9**. A comparative analysis of the bound pose of **8j** and Ulixertinib revealed that the designed molecules occupy the hydrophobic pocket similar to Ulixertinib, an additional aromatic side flank present in the designed molecules occupy the small hydrophobic pocket, lined with Ile31 and Val39, tunnelling out of the ATP-binding site (**Figure 4.10**). Variations in the bound pose of the designed molecules and changes in the protein conformation during the 100ns simulation time period clearly indicated that except slight deviations, consistent contacts with hinge region residues were preserved in the complex (**Figure 4.11**). Another important observation made during the post-MD analysis of the selected compounds was the interactions of the designed molecules with hydrophobic amino acid residues (Ile31, Gly32, Ala35, Val39 and Leu107) which forms one of the side walls of the binding pocket and make critical contribution to the binding affinity of the ligands, as disclosed in our previous study. MM-GBSA score calculations and the obtained scores clearly indicated that binding affinity correlated well with hydrophobic interactions between designed compounds and crucial amino acid residues, ranging from -44.49 to -34.01 kcal/mol (**Table 4.9**). Further we analyzed the contribution of key residues in the binding energy by reviewing the decomposition data. Residues such as Leu107, Met108 and Lys114 contributed favourably in the formation of the complex. Therefore, these top molecules (fifteen) were forwarded to synthesis and ERK2 inhibitory assay.



**Figure 4.8.** RMSD plot of **8j** in complex with ERK2 for the time period of 100 ns.

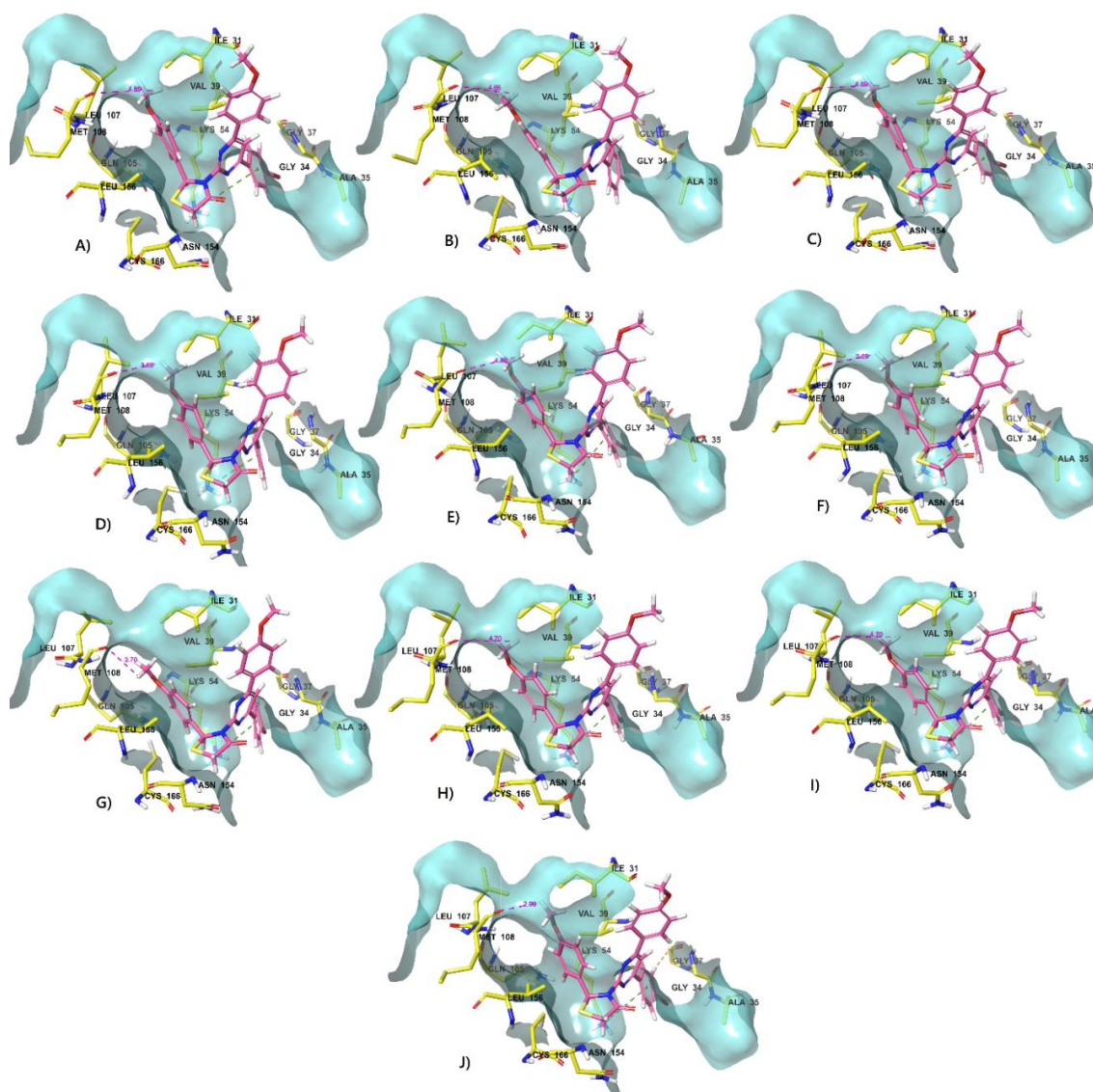


**Figure 4.9.** 3D interaction map of **8j** in the binding pocket of ERK2 after simulation period of 100ns.



**Figure 4.10.** An overlapped pose of **8j** (yellow) and Ulixertinib (green) in the ATP-binding pocket of ERK2.

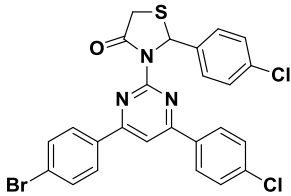
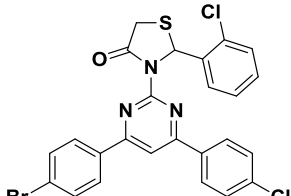
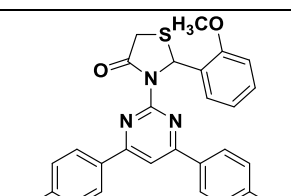
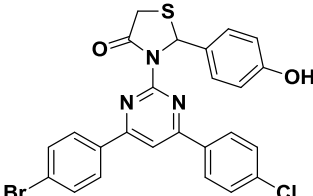
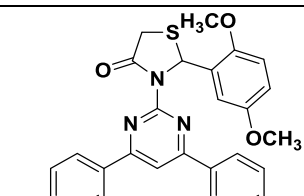
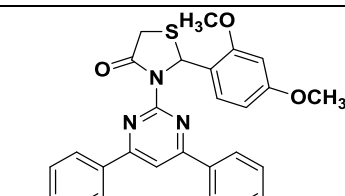


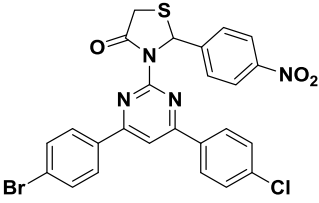
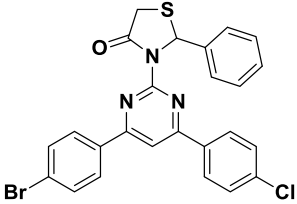
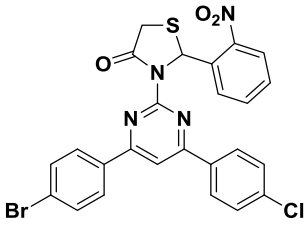
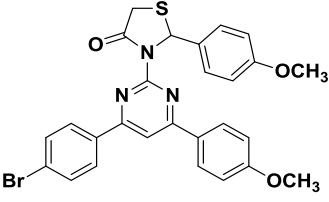
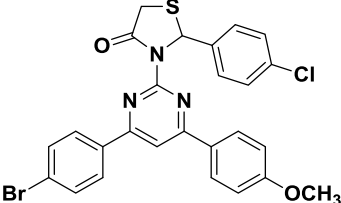
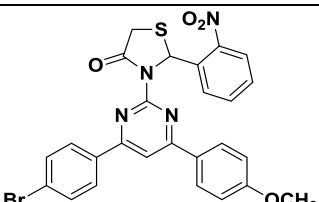


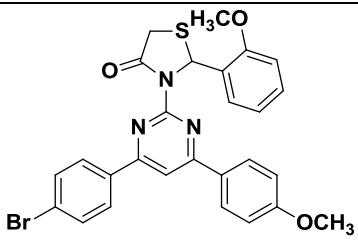
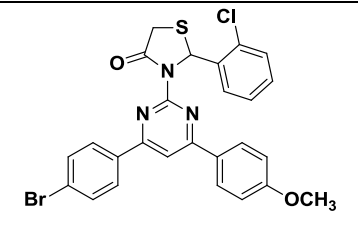
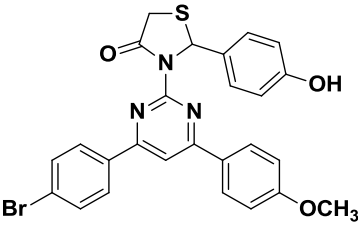
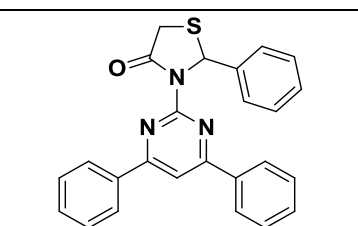
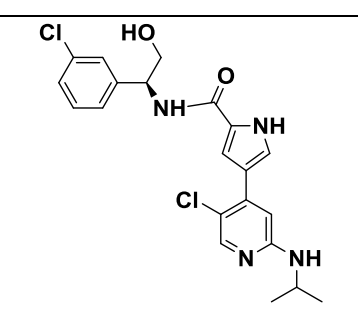
**Figure 4.11.** Various poses at each 10ns time frames from 0 to 100 ns for MD of **8j** in the ATP-binding site of ERK2. Distance between hinge region residues and  $-OCH_3$  is also provided in each snapshot. A) at 10ns; B) at 20ns; C) at 30ns; D) at 40ns; E) at 50ns; F) at 60ns; G) at 70ns; H) at 80ns; I) at 90ns; J) at 100ns.



Table 4.8. Docking score and binding affinity score of the designed compounds.

S. No.	Compound	2D-structure	Docking Score (Glide score)	MM-GBSA binding energy (Kcal/mol)
1.	8a		-6.57	-43.33
2.	8b		-5.334	-37.63
3.	8c		-4.547	-37.56
4.	8d		-4.903	-43.87
5.	8e		-5.016	-42.1
6.	8f		-5.465	-34.5

7.	<b>8g</b>		-5.938	-34.85
8.	<b>8h</b>		-5.361	-34.63
9.	<b>8i</b>		-4.696	-34.01
10.	<b>8j</b>		-5.505	-44.49
11.	<b>8k</b>		-5.262	-37.34
12.	<b>8l</b>		-5.418	-38.87

13.	<b>8m</b>		-5.102	-42.04
14.	<b>8n</b>		-5.377	-37.43
15.	<b>8o</b>		-5.561	-41.07
16.	<b>Ligand 8</b>		-4.616	-33.06
17.	<b>Ulixertinib</b>		-7.267	-57.43

**Table 4.9.** Various component of the MM-GBSA binding score for designed compounds.

Comp ID	dG Bind	dG Bind Coulomb	dG Bind Covalent	dG Bind Hbond	dG Bind Lipo	dG Bind Packing	dG Bind SelfCont	dG Bind Solv GB	dG Bind vdW
8a	-43.33	-8.25	5.5	-0.14	-23.67	-0.09	0	26.81	-43.48
8b	-37.63	-14.59	3.42	-0.73	-17.86	-0.63	0	36.27	-43.51
8c	-37.56	-20.39	1.6	-0.89	-13.89	-0.11	0	38.06	-41.94
8d	-43.87	-13.19	7.02	-0.5	-17.58	-0.13	0	32.3	-51.78
8e	-42.1	-1.51	2.27	-0.09	-16.47	-0.13	0	28.17	-54.33
8f	-34.5	-13.57	4.53	-1	-15.48	-0.77	0	37.58	-45.79
8g	-34.85	-4.97	4.29	-1.19	-16.94	-0.09	0	34.47	-50.42
8h	-34.63	-5.89	8.85	-0.14	-17.21	-0.52	0	36.47	-56.2
8i	-34.01	2.32	7.06	-0.31	-15.96	-0.18	0	27.23	-54.18
8j	-44.49	-10.08	6.66	-0.71	-17.51	-0.25	0	24.03	-46.62
8k	-37.34	-11.18	8.16	-0.24	-20	-0.01	0	31.25	-45.32
8l	-38.87	0.99	4.98	-0.23	-17.4	-0.15	0	28.47	-55.53
8m	-42.04	-1.35	2.17	-0.19	-16.17	-0.03	0	28.07	-54.23
8n	-37.43	-11.37	8.26	-0.34	-19.9	-0.11	0	31.4	-45.37
8o	-41.07	-1.78	3.57	-1.19	-15.37	-0.2	0	28.34	-54.23
Ulixertinib	-57.43	-21.11	0.86	-2.49	-22.87	-0.01	0	48.29	-60.11

Finally, to estimate the drug-likeness of the designed compounds, some of their physicochemical properties were calculated. Almost all the compounds possess favorable drug-likeness profile with maximum two violations per molecule for Lipinski's rule of five (**Table 4.10.**). For most of the compounds, logP value was found to be < six along with hydrogen bond donor score of < five. Except a few, in Qikprop predictions, all the designed molecules were predicted to possess 100% human oral absorption. The QP PCaco values suggested a need to improve the permeability profile of the compounds and hence these compounds can be further optimized to improve cell membrane permeability and optimize drug-like profile.

Table 4.10. Physicochemical properties of the designed compounds (8a-8o)

S. No.	Comp ID	Mol. MW	QP logPo/w	HB donor	HB acceptor	QP PCaco	QP logK <sub>hsa</sub>	QPlog HERG	Rule of Five
1.	8a	557.291	6.459	0	5	4476.178	0.918	-5.292	2
2.	8b	557.291	6.294	0	5	4755.123	0.881	-5.401	2
3.	8c	552.872	6.041	0	6	4954.441	0.754	-4.103	2
4.	8d	538.845	5.432	1	6	1350.084	0.82	-5.336	2
5.	8e	582.898	6.308	0	7	5653.142	0.794	-5.828	2
6.	8f	582.898	6.047	0	7	5235.749	0.698	-5.842	2
7.	8g	567.843	5.198	0	6	562.547	0.684	-5.318	2
8.	8h	522.846	5.968	0	5	4449.717	0.795	-5.412	2
9.	8i	567.843	5.554	0	6	1536.478	0.7	-5.431	2
10.	8j	548.453	5.576	0	7	4404.474	0.62	-4.259	2
11.	8k	552.872	6.058	0	6	4458.389	0.783	-4.384	2
12.	8l	563.424	4.778	0	7	1495.559	0.412	-4.799	1
13.	8m	548.453	5.956	0	7	4325.249	0.639	-4.422	2
14.	8n	552.872	6.115	0	6	4239.583	0.776	-4.349	2
15.	8o	535.048	6.478	1	5	1548.484	0.825	-5.154	2
	Range/Recommended value	130.0-725.0	-2.0-6.5	0.0-6.0	2.0-20.0	<25 poor, >500 great	-1.5-1.5	concern below -5	Maximum is 4

#### 4.1.3. Exploring effect of ring size increase on binding affinity of hit (Ligand 8) derivatives (Formula-II)

As a second round of optimization, a library of more than 100 derivatives (Table 4.11.) were designed by increasing the ring size of the five-membered ring system

(thiazolidin-4-one) present in Ligand **8**, to a six-membered ring system (1,3-thiazinan-4-one), to explore the binding pocket occupancy and its effect in the inhibition of ERK2 (**Figure 4.12.**). While the diverse hydrophobic substituents were also incorporated at different sites on the core structure, as done previously and subjected them to *in silico* evaluation to filter out derivatives with improved binding affinity for ERK2, in comparison to five-membered molecules (**8a-8o**), followed by their synthesis, characterization and evaluation of their *in-vitro* potential as ERK2 inhibitors.

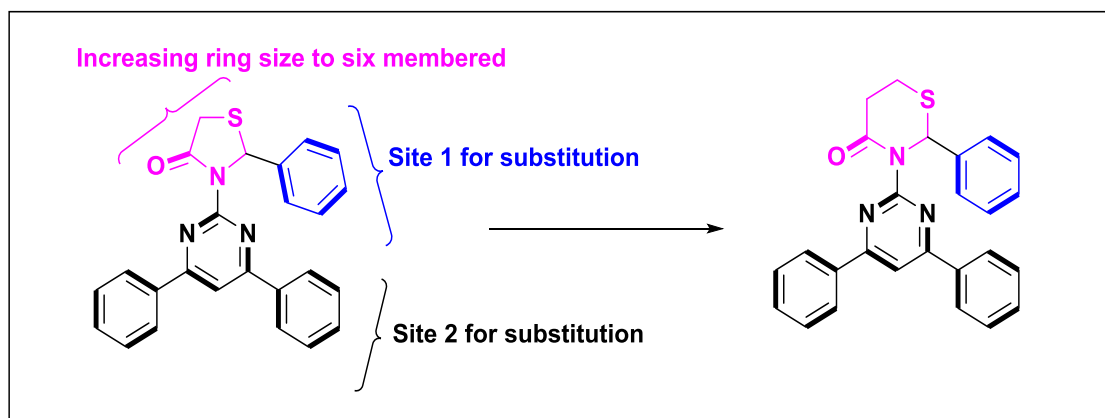


**Figure 4.12.** Increasing ring size of five-membered system in Ligand **8**, along with previous substitutions to generate an *in-house* library.

Similar screening parameters were considered for the second set of molecules to identify the top hits, which were then forwarded for synthesis. Briefly, various analogues with similar substitutions as first library with increased ring size were sketched and docked in the co-crystallized protein structure of ERK2. Derivatives maintaining the essential interactions in the binding pocket of ERK2, were screened and subjected to MD simulations for 100 ns and binding affinity analysis. The designed molecules which retained key interactions and maintained a stable complex with the ERK2 were then forwarded for the determination of binding affinity (MM-GBSA score). Out of all derivatives present in the library, a total 15 molecules were

found to possess similar docking scores (glide scores) in comparison to the lead (Ligand **8**), ranging from 7.18–4.33 Kcal/mol (Table 4.11.). After the MD simulation of 100 ns, the RMSD values were determined to study the stability of the complexes. The RMSD plot of the designed compound (**10h**) in complex along with native protein backbone atoms revealed complexes to be fairly stable. The graph for the same, plotted against time, is shown in Figure 4.13.

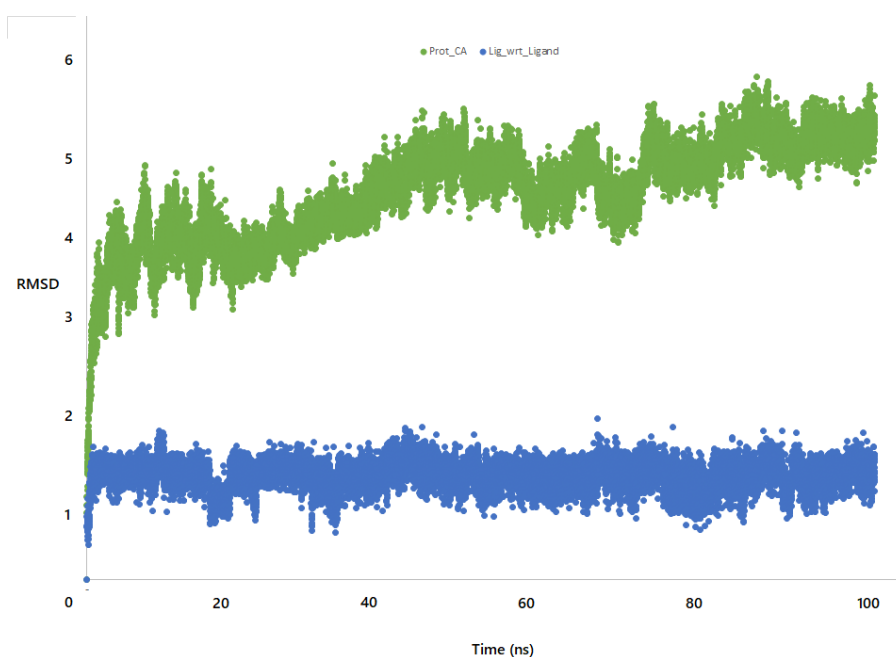


**Figure 4.13.** RMSD plot of **10h** in complex with ERK2 for the time period of 100 ns.

Upon establishing the stability of the complexes, interaction plot of the designed molecules in the binding pocket of ERK2 were studied to generalize their binding mode. It revealed that in almost all the complexes the 1,3-thiazinan-4-one nucleus protruded outwards pushing the di-aryl pyrimidine assembly into the pocket leading to tight packing of the designed molecules. The -Cl on one of the aryl ring formed halogen bond with Asp106, while Lys54 formed  $\pi$ -cation interaction with the other aryl ring. Additionally, in case of some of the selected compounds, pyrimidine nucleus acts as H-bond acceptor for crucial amino acid residue Lys54. While, in some

of the designed molecules, -Br on the aryl ring interacted with hydrophobic amino acid residues including Tyr36 *via* halogen bond. Importantly, the top hits retained key interactions network in the binding pocket of ERK2 which involved catalytic domain amino acid such as Met108, Lys114, Leu107, Lys54, Gly34, Asp106, Ser153, Ala35, Gly37, Ile56 of ERK2, after the complete simulation run, suggesting putative inhibitory potential of the screened hits. 3D interaction diagram for one of the selected molecules (10h) in the binding pocket of ERK2 is shown in **Figure 4.14**. A comparative analysis of the top hits revealed that although increasing the ring size did tighten the fitting in the pocket, it completely altered the interaction network of the derivatives from the five membered predecessors (**Figure 4.15**). Another important observation made during the post-MD analysis of the selected compounds was the interactions of the designed molecules with hydrophobic amino acid residues (Ile31, Glu33, Gly34, Ala35, Val39 and Leu107) which forms one of the side walls of the binding pocket and make critical contribution to the binding affinity of the ligands, as disclosed in our previous study. Overall, all the top molecules were found to maintain varied but significant levels of interaction with these crucial hydrophobic amino acid residues along with key interactions with Met108 and Lys54. Accordingly, these top molecules were forwarded to synthesis and ERK2 inhibitory assay.

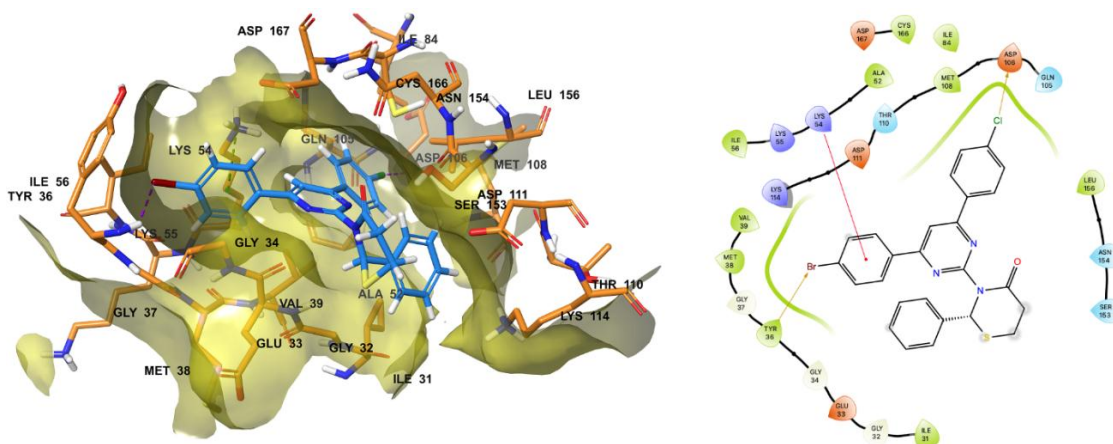


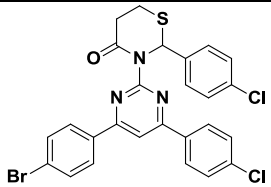
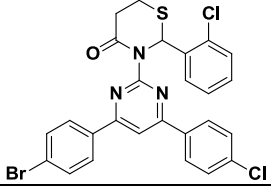
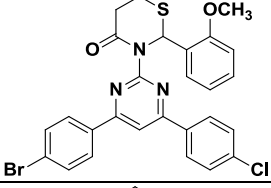
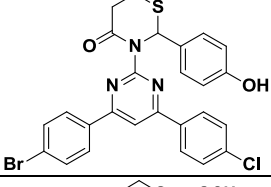
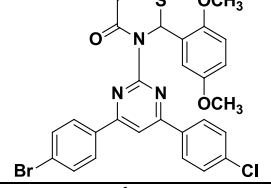
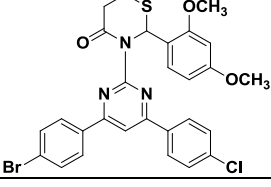
**Figure 4.14.** 3D interaction diagram of top hits, **10h** in the catalytic domain of ERK2.

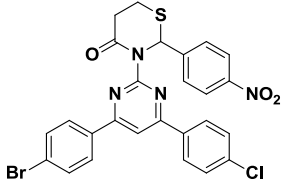
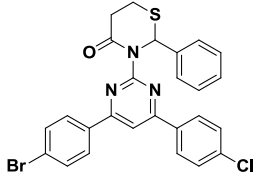
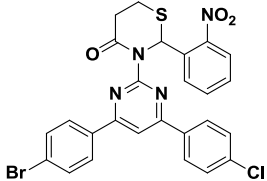
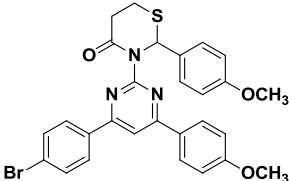
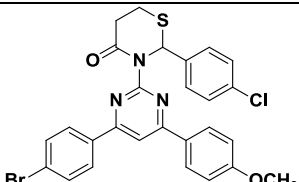
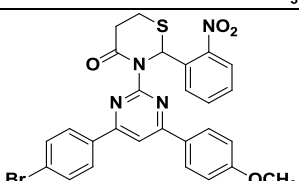
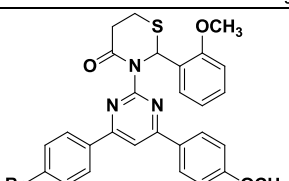
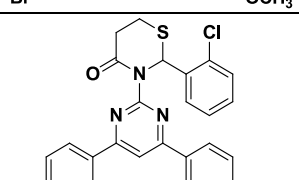


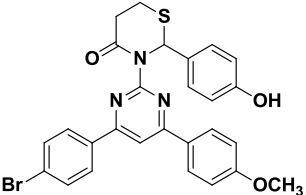


(Table 4.11.). Further we analyzed the contribution of key residues in the binding energy by reviewing the decomposition data (Table 4.12.). Residues such as Glu33, Gly34, Ala35, and Lys54 contributed favourably in the formation of the complex.

**Table 4.11.** Designed compounds with their binding energies and predicted activity.

S.No.	Compound	2D-structure	Docking Score (Glide score)	MM-GBSA binding energy (Kcal/mol)
1.	<b>10a</b>		-5.612	-40.23
2.	<b>10b</b>		-4.33	-45.93
3.	<b>10c</b>		-6.861	-39.58
4.	<b>10d</b>		-7.067	-53.45
5.	<b>10e</b>		-5.061	-44.88
6.	<b>10f</b>		-6.89	-48.45

7.	<b>10g</b>		-6.714	-52.34
8.	<b>10h</b>		-7.189	-54.68
9.	<b>10i</b>		-6.696	-44.89
10.	<b>10j</b>		-5.379	-37.52
11.	<b>10k</b>		-5.891	-41.09
12.	<b>10l</b>		-5.517	-42.2
13.	<b>10m</b>		-6.695	-42.13
14.	<b>10n</b>		-4.884	-37.79

15.	<b>10o</b>		-6.195	-49.35
-----	------------	---	--------	--------

**Table 4.12.** Various component of the MM-GBSA binding score for designed compounds.

Comp ID	dG Bind	dG Bind Coulomb	dG Bind Covalent	dG Bind Hbond	dG Bind Lipo	dG Bind Packing	dG Bind SelfCont	dG Bind Solv GB	dG Bind vdW
<b>10a</b>	-40.23	1.59	10.52	-0.004	-22.91	-0.06	0.0	30.55	-59.91
<b>10b</b>	-45.93	-16.27	3.42	-0.75	-13.83	-0.33	0.0	36.21	-54.36
<b>10c</b>	-39.58	-12.80	10.61	-0.67	-16.97	-0.03	0.0	34.58	-54.28
<b>10d</b>	-53.45	-19.23	10.92	-0.48	-18.05	-0.04	0.0	31.59	-57.14
<b>10e</b>	-44.88	-20.83	10.18	-0.92	-14.06	-0.07	0.0	37.92	-57.08
<b>10f</b>	-48.45	-18.86	13.66	-0.74	-18.70	-0.03	0.0	36.09	-59.86
<b>10g</b>	-52.34	-5.37	10.98	-0.69	-22.01	-0.04	0.0	24.74	-60.69
<b>10h</b>	-54.68	-18.43	11.59	-0.004	-21.87	-0.04	0.0	30.90	-56.69
<b>10i</b>	-44.89	-14.94	7.49	-0.48	-19.48	-0.008	0.0	34.91	-52.37
<b>10j</b>	-37.52	-9.87	10.13	-0.48	-17.97	-0.03	0.0	37.74	-57.02
<b>10k</b>	-41.09	-14.69	10.70	-0.43	-18.34	-0.04	0.0	39.49	-57.76
<b>10l</b>	-42.2	-6.97	4.46	-0.82	-16.08	-0.26	0.0	28.33	-52.80
<b>10m</b>	-42.13	-6.81	4.37	-0.71	-15.99	-0.21	0.0	30.45	-54.67
<b>10n</b>	-37.79	-10.24	10.28	-0.43	-18.37	-0.05	0.0	38.26	-56.92
<b>10o</b>	-49.35	-19.76	13.16	-0.94	-18.85	-0.06	0.0	36.1	-59.99
<b>Ulixer tinib</b>	-57.43	-21.11	0.86	-2.49	-22.87	-0.01	0	48.29	-60.11

Finally, the drug-likeness of the designed compounds was estimated via calculation of their physicochemical properties. Almost all the compounds possess decent drug-likeness profile with maximum two violations per molecule for Lipinski's rule of five (Table 4.13.). For most of the compounds, logP value was found to be < six along with hydrogen bond donor score of < five. Except a few, in Qikprop predictions, all the designed molecules were predicted to possess 100% human oral absorption.

Table 4.13. Physicochemical properties of the designed compounds (10a-10o)

S. No.	Comp ID	Mol. MW	QP logPo/w	HB donor	HB acceptor	QP PCaco	QP logKhsa	Percent Oral Absorption	Rule of Five
1.	10a	571.318	7.127	0	6	3554.468	1.257	100	2
2.	10b	571.318	7.120	0	6	4070.251	1.250	100	2
3.	10c	566.899	6.877	0	6	3859.445	1.165	100	2
4.	10d	552.872	5.979	1	6	1323.496	1.063	91.91	2
5.	10e	596.925	6.625	0	7	4371.932	0.989	100	2
6.	10f	596.925	7.119	0	7	4621.751	1.169	100	2
7.	10g	581.870	5.927	0	6	566.143	1.007	85	2
8.	10h	536.873	6.664	0	5	3630.837	1.139	100	2
9.	10i	581.870	5.943	0	6	1260.190	0.905	91	2
10.	10j	562.480	6.378	0	7	4261.881	0.973	100	2
11.	10k	566.899	6.680	0	6	4157.650	1.093	100	2
12.	10l	577.451	5.519	0	7	783.817	0.831	85.14	2
13.	10m	562.480	6.524	0	7	3584.254	1.011	100	2
14.	10n	566.899	6.165	0	6	4652.543	0.913	100	2
15.	10o	549.254	7.132	1	6	4361.143	1.245	100	2
	<b>Range /Recommended value</b>	130.0-725.0	-2.0-6.5	0.0-6.0	2.0-20.0	<25 poor, >500 great	-1.5-1.5	>80% is high, <25% is poor	Maximum is 4

## 4.2. RESULTS OF SYNTHESIS

As mentioned above, 30 hits obtained from optimizing both hydrophobic substituents and ring size of the virtual hit, identified via scaffold hopping and fragment-based drug discovery-based hybrid virtual screening protocol, were carried forward to

synthesis and characterization. The obtained hits constituted of two major classes of fused heterocycles: thiazolidinone-pyrimidine and thiazinanone-pyrimidine.

#### 4.2.1. List of synthesized compounds

List of all the compounds pertaining to two schemes is given in the **Table 4.14**. IUPAC names of the synthesized compounds were given by applying general rules of heterocyclic nomenclature.

**Table 4.14. IUPAC names of synthesized compounds.**

Sr No.	Code	IUPAC Name
1.	<b>8a</b>	3-(4-(4-bromophenyl)-6-(4-chlorophenyl)pyrimidin-2-yl)-2-(4-chlorophenyl)thiazolidin-4-one
2.	<b>8b</b>	3-(4-(4-bromophenyl)-6-(4-chlorophenyl)pyrimidin-2-yl)-2-(2-chlorophenyl)thiazolidin-4-one
3.	<b>8c</b>	3-(4-(4-bromophenyl)-6-(4-chlorophenyl)pyrimidin-2-yl)-2-(2-methoxyphenyl)thiazolidin-4-one
4.	<b>8d</b>	3-(4-(4-bromophenyl)-6-(4-chlorophenyl)pyrimidin-2-yl)-2-(4-hydroxyphenyl)thiazolidin-4-one
5.	<b>8e</b>	3-(4-(4-bromophenyl)-6-(4-chlorophenyl)pyrimidin-2-yl)-2-(2,5-dimethoxyphenyl)thiazolidin-4-one
6.	<b>8f</b>	3-(4-(4-bromophenyl)-6-(4-chlorophenyl)pyrimidin-2-yl)-2-(2,4-dimethoxyphenyl)thiazolidin-4-one
7.	<b>8g</b>	3-(4-(4-bromophenyl)-6-(4-chlorophenyl)pyrimidin-2-yl)-2-(4-nitrophenyl)thiazolidin-4-one
8.	<b>8h</b>	3-(4-(4-bromophenyl)-6-(4-chlorophenyl)pyrimidin-2-yl)-2-

---

		phenylthiazolidin-4-one
9.	<b>8i</b>	3-(4-(4-bromophenyl)-6-(4-chlorophenyl)pyrimidin-2-yl)-2-(2-nitrophenyl)thiazolidin-4-one
10.	<b>8j</b>	3-(4-(4-bromophenyl)-6-(4-methoxyphenyl)pyrimidin-2-yl)-2-(4-methoxyphenyl)thiazolidin-4-one
11.	<b>8k</b>	3-(4-(4-bromophenyl)-6-(4-methoxyphenyl)pyrimidin-2-yl)-2-(4-chlorophenyl)thiazolidin-4-one
12.	<b>8l</b>	3-(4-(4-bromophenyl)-6-(4-methoxyphenyl)pyrimidin-2-yl)-2-(2-nitrophenyl)thiazolidin-4-one
13.	<b>8m</b>	3-(4-(4-bromophenyl)-6-(4-methoxyphenyl)pyrimidin-2-yl)-2-(2-methoxyphenyl)thiazolidin-4-one
14.	<b>8n</b>	3-(4-(4-bromophenyl)-6-(4-methoxyphenyl)pyrimidin-2-yl)-2-(2-chlorophenyl)thiazolidin-4-one
15.	<b>8o</b>	3-(4-(4-bromophenyl)-6-(4-methoxyphenyl)pyrimidin-2-yl)-2-(4-hydroxyphenyl)thiazolidin-4-one
16.	<b>10a</b>	3-(4-(4-bromophenyl)-6-(4-chlorophenyl)pyrimidin-2-yl)-2-(4-chlorophenyl)-1,3-thiazinan-4-one
17.	<b>10b</b>	3-(4-(4-bromophenyl)-6-(4-chlorophenyl)pyrimidin-2-yl)-2-(2-chlorophenyl)-1,3-thiazinan-4-one
18.	<b>10c</b>	3-(4-(4-bromophenyl)-6-(4-chlorophenyl)pyrimidin-2-yl)-2-(2-methoxyphenyl)-1,3-thiazinan-4-one
19.	<b>10d</b>	3-(4-(4-bromophenyl)-6-(4-chlorophenyl)pyrimidin-2-yl)-2-(4-hydroxyphenyl)-1,3-thiazinan-4-one
20.	<b>10e</b>	3-(4-(4-bromophenyl)-6-(4-chlorophenyl)pyrimidin-2-yl)-2-(2,5-

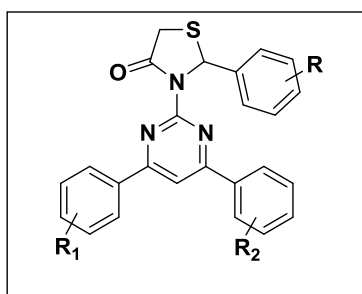
---

		dimethoxyphenyl)-1,3-thiazinan-4-one
21.	<b>10f</b>	3-(4-(4-bromophenyl)-6-(4-chlorophenyl)pyrimidin-2-yl)-2-(2,4-dimethoxyphenyl)-1,3-thiazinan-4-one
22.	<b>10g</b>	3-(4-(4-bromophenyl)-6-(4-chlorophenyl)pyrimidin-2-yl)-2-(4-nitrophenyl)-1,3-thiazinan-4-one
23.	<b>10h</b>	3-(4-(4-bromophenyl)-6-(4-chlorophenyl)pyrimidin-2-yl)-2-phenyl-1,3-thiazinan-4-one
24.	<b>10i</b>	3-(4-(4-bromophenyl)-6-(4-chlorophenyl)pyrimidin-2-yl)-2-(2-nitrophenyl)-1,3-thiazinan-4-one
25.	<b>10j</b>	3-(4-(4-bromophenyl)-6-(4-methoxyphenyl)pyrimidin-2-yl)-2-(4-methoxyphenyl)-1,3-thiazinan-4-one
26.	<b>10k</b>	3-(4-(4-bromophenyl)-6-(4-methoxyphenyl)pyrimidin-2-yl)-2-(4-chlorophenyl)-1,3-thiazinan-4-one
27.	<b>10l</b>	3-(4-(4-bromophenyl)-6-(4-methoxyphenyl)pyrimidin-2-yl)-2-(2-nitrophenyl)-1,3-thiazinan-4-one
28.	<b>10m</b>	3-(4-(4-bromophenyl)-6-(4-methoxyphenyl)pyrimidin-2-yl)-2-(2-methoxyphenyl)-1,3-thiazinan-4-one
29.	<b>10n</b>	3-(4-(4-bromophenyl)-6-(4-methoxyphenyl)pyrimidin-2-yl)-2-(2-chlorophenyl)-1,3-thiazinan-4-one
30.	<b>10o</b>	3-(4-(4-bromophenyl)-6-(4-methoxyphenyl)pyrimidin-2-yl)-2-(4-hydroxyphenyl)-1,3-thiazinan-4-one



### 4.2.2. Characterization of compounds pertaining to Formula-I (8a-8o)

After the synthesis of designed compounds, characterization of the compounds was done *via*  $^1\text{H-NMR}$ ,  $^{13}\text{C}$  NMR and Mass spectrometry. The peaks in spectral analysis were assigned to structural features of synthesized compounds using various literature sources (Silverstein and Bassler 1962; Kemp 1991; Pavia, Lampman et al. 2014). The physical properties of the compounds pertaining to formula-I have been given in **Table 4.15**. In general, the IR spectrum for the thiazolidinone-pyrimidine derivatives exhibited a characteristic absorption band for C=O from  $\sim 1705$  to  $\sim 1715\text{ cm}^{-1}$  and absorption bands for aromatic C=N from  $\sim 1690$  to  $\sim 1550\text{ cm}^{-1}$  were also observed. The  $^1\text{H-NMR}$  spectrum for all the thiazolidinone-pyrimidine derivatives showed characteristic singlet from  $\sim 7.7$  to  $\sim 8.2$  ppm for one proton presents in the pyrimidine nucleus; the value deviated slightly in different derivatives because of the electronic nature of the substituents. Most of the aromatic protons retained their pattern throughout the series and appeared at similar values from  $\sim 6.5$  to  $\sim 7.9$  ppm. Overlapped doublets, appearing as multiplet of two protons between  $\sim 3.3$  to  $\sim 4.0$  ppm for  $-\text{CH}_2$  confirmed the formation of the thiazolidinone ring. Accordingly, mass spectra also showed the presence of the expected fragmentation pattern with quasi-ion peaks at the required  $m/z$  values. Characteristic  $M + 2$  and  $M + 4$  values were also recorded in each mass spectrum due to presence of  $-\text{Cl}$  and  $-\text{Br}$  atoms throughout the series.



Formula-I

**Table 4.15.** Physical characteristics of synthesized compounds pertaining to Formula I (8a-8o).

Comp. Code	R	R <sub>1</sub>	R <sub>2</sub>	Color	R <sub>f</sub> value <sup>a</sup> Hexane: EtAc	% Yield	Melting point <sup>b</sup> (°C)
8a	4-Cl	Br	Cl	Yellow	0.31	30.5%	212–214
8b	2-Cl	Br	Cl	Light yellow	0.35	32.6%	210–212
8c	2-OCH <sub>3</sub>	Br	Cl	Yellow	0.38	32.1%	195–197
8d	4-OH	Br	Cl	Yellow	0.33	40.6%	217–219
8e	2,5-di-OCH <sub>3</sub>	Br	Cl	Yellow	0.42	40.8%	190–192
8f	2,4-di-OCH <sub>3</sub>	Br	Cl	Yellow	0.42	35.8%	191–193
8g	4-NO <sub>2</sub>	Br	Cl	Yellow	0.43	40.6%	203–205
8h	H	Br	Cl	Light yellow	0.40	20.2%	180–182
8i	2-NO <sub>2</sub>	Br	Cl	Light yellow	0.44	24.5%	206–208
8j	4-OCH <sub>3</sub>	Br	OCH <sub>3</sub>	Yellow	0.39	30.5%	186–188
8k	4-Cl	Br	OCH <sub>3</sub>	Yellow	0.36	22.5%	196–198
8l	2-NO <sub>2</sub>	Br	OCH <sub>3</sub>	Yellow	0.38	32.5%	188–190
8m	2-OCH <sub>3</sub>	Br	OCH <sub>3</sub>	Yellow	0.38	32.5%	188–190
8n	2-Cl	Br	OCH <sub>3</sub>	Yellow	0.38	32.5%	188–190

<b>8o</b>	4-OH	Br	OCH <sub>3</sub>	Yellow	0.38	32.5%	188-190
-----------	------	----	------------------	--------	------	-------	---------

<sup>a</sup>EtAc: ethyl acetate

<sup>b</sup>Determined melting points are uncorrected.

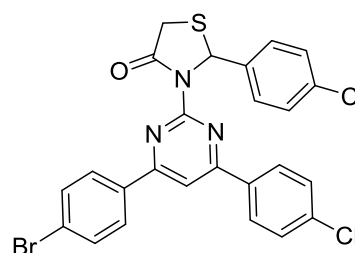
### 4.2.3. Compound sheets

#### 4.2.3.1. 3-(4-(4-bromophenyl)-6-(4-chlorophenyl)pyrimidin-2-yl)-2-(4-chlorophenyl)thiazolidin-4-one (**8a**)

**Yield**, 30.5 %

**Molecular Weight**, 557.29

**Molecular Formula**, C<sub>25</sub>H<sub>16</sub>BrCl<sub>2</sub>N<sub>3</sub>OS



**Procedure:** The intermediate **5** (0.001 mol), in 8 ml toluene and catalytic amount of glacial acetic acid, was treated with 4-chlorobenzaldehyde (1 eq.), as per the procedure given in section 3.2.2.3, to yield desired product **8a**. Further column chromatography (Silica gel # 60-120; Hexane:Ethyl acetate : : 80: 20) was performed to afford pure compound.

**State & colour:** Yellow solid

**R<sub>f</sub> value** 0.31

**Melting Point:** 212-214°C

**MS (+ESI) m/z** 555.97 [M+H]<sup>+</sup>,  
557.96 [M+2+H]<sup>+</sup>

**IR (cm<sup>-1</sup>)** 1717 (C=O), 1659 (C=N), 1630 (C=N), 1589 (C=N)

**<sup>1</sup>H NMR (400 MHz, CDCl<sub>3</sub>)** 8.21 (s, 1H), 7.93–7.91 (m, 2 H), 7.82–7.80 (m, 2 H),  
7.60–7.58 (m, 2 H), 7.35–7.21 (m, 6 H), 3.92–3.84 (m, 2 H)

**<sup>13</sup>C NMR (100 MHz,** 168.99, 160.63, 160.26, 157.04, 136.91, 135.26, 134.36,

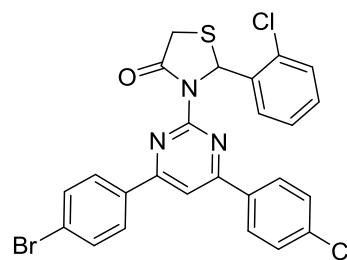
CDCl<sub>3</sub>) 133.97, 133.51, 131.55, 129.77, 129.49, 129.31, 129.28,  
128.79, 122.82, 107.59, 63.03, 33.91

**4.2.3.2. 3-(4-(4-bromophenyl)-6-(4-chlorophenyl)pyrimidin-2-yl)-2-(2-chlorophenyl) thiazolidin-4-one (8b)**

**Yield,** 32.6 %

**Molecular Weight,** 557.29

**Molecular Formula,** C<sub>25</sub>H<sub>16</sub>BrCl<sub>2</sub>N<sub>3</sub>OS



**Procedure:** In 8 ml toluene and catalytic amount of glacial acetic acid, intermediate 5 (0.001 mol), was treated with 2-chlorobenzaldehyde (1 eq.), as per the procedure given in section 3.2.2.3, to yield desired product **8b**. Additionally, column chromatography (Silica gel # 60-120; Hexane:Ethyl acetate : : 80: 20) was performed to afford pure compound.

**State & colour:** Light yellow solid

**R<sub>f</sub> value** 0.35

**Melting Point:** 210-212°C

**MS (+ESI) m/z** 555.97 [M+H]<sup>+</sup>,  
557.96 [M+2+H]<sup>+</sup>

**IR (cm<sup>-1</sup>)**

1721 (C=O), 1635 (C=N), 1611 (C=N), 1572 (C=N)

**<sup>1</sup>H NMR (400 MHz,**

8.21 (s, 1H), 7.93–7.91 (m, 2 H), 7.82–7.80 (m, 2 H),

CDCl<sub>3</sub>)

7.60–7.58 (m, 2 H), 7.45–7.43 (m, 1H), 7.35–7.27 (m, 5  
H), 3.91– 3.84 (m, 2 H)

**<sup>13</sup>C NMR (100 MHz,**

169.16, 160.63, 160.26, 156.69, 137.21, 135.26, 133.97,

CDCl<sub>3</sub>)

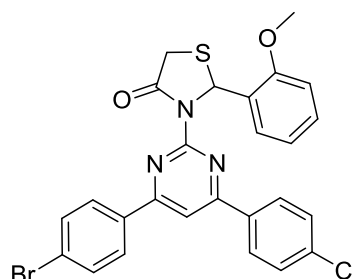
133.51, 132.48, 131.55, 130.36, 129.82, 129.77, 129.67,  
129.49, 128.79, 128.09, 122.82, 107.59, 58.52, 33.82

4.2.3.3. 3-(4-(4-bromophenyl)-6-(4-chlorophenyl)pyrimidin-2-yl)-2-(2-methoxyphenyl)thiazolidin-4-one (8c)

Yield, 32.1 %

Molecular Weight, 552.87

Molecular Formula, C<sub>26</sub>H<sub>19</sub>BrClN<sub>3</sub>O<sub>2</sub>S



**Procedure:** In 8 ml toluene and catalytic amount of glacial acetic acid, intermediate 5 (0.001 mol), was treated with 2- methoxybenzaldehyde (1 eq.), as per the procedure given in section 3.2.2.3, to yield desired product 8c. Additionally, column chromatography (Silica gel # 60-120; Hexane:Ethyl acetate : : 80: 20) was performed to afford pure compound.

**State & colour:** Yellow solid

**R<sub>f</sub> value:** 0.38

**Melting Point:** 195-197°C

**MS (+ESI) m/z:** 552.02 [M+H]<sup>+</sup>,  
554.01 [M+2+H]<sup>+</sup>

**IR (cm<sup>-1</sup>)** 1721 (C=O), 1635 (C=N), 1611 (C=N), 1572 (C=N)

**<sup>1</sup>H NMR (400 MHz, CDCl<sub>3</sub>)** 8.21 (s, 1H), 7.93–7.91 (m, 2 H), 7.82–7.80 (m, 2 H),  
7.60–7.58 (m, 2 H), 7.45–7.43 (m, 1H), 7.13–7.08 (m, 2 H),  
6.95–6.93 (m, 1H), 3.92–3.82 (m, 5 H)

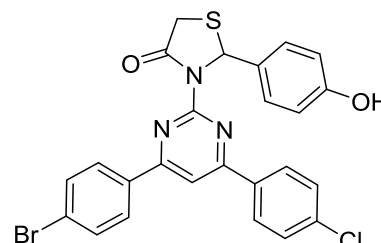
**<sup>13</sup>C NMR (100 MHz, CDCl<sub>3</sub>)** 169.17, 160.63, 160.25, 157.51, 156.88, 135.26, 133.97,  
133.51, 131.55, 129.77, 129.49, 129.35, 128.79, 128.75,  
126.63, 122.82, 122.38, 112.76, 107.59, 56.45, 55.62,  
33.82

4.2.3.4. 3-(4-(4-bromophenyl)-6-(4-chlorophenyl)pyrimidin-2-yl)-2-(4-hydroxyphenyl)thiazolidin-4-one (**8d**)

Yield, 40.6 %

Molecular Weight, 538.84

Molecular Formula, C<sub>25</sub>H<sub>17</sub>BrClN<sub>3</sub>O<sub>2</sub>S



**Procedure:** In 8 ml toluene and catalytic amount of glacial acetic acid, intermediate 5 (0.001 mol), was treated with 4-hydroxybenzaldehyde (1 eq.), as per the procedure given in section 3.2.2.3, to yield desired product **8d**. Additionally, column chromatography (Silica gel # 60-120; Hexane:Ethyl acetate : : 80: 20) was performed to afford pure compound.

**State & colour:** Yellow solid

**R<sub>f</sub> value:** 0.33

**Melting Point:** 217-219°C

**MS (+ESI) m/z:** 540.54 [M+H]<sup>+</sup>,  
542.51 [M+2+H]<sup>+</sup>

**IR (cm<sup>-1</sup>)** 1721 (C=O), 1635 (C=N), 1611 (C=N), 1572 (C=N)

**<sup>1</sup>H NMR (400 MHz,** 8.21 (s, 1H), 7.93–7.91 (m, 2 H), 7.82–7.80 (m, 2 H),

**CDCl<sub>3</sub>)** 7.60–7.58 (m, 2 H), 7.45–7.43 (m, 1H), 7.35–7.27 (m, 5 H), 3.91– 3.84 (m, 2 H)

**<sup>13</sup>C NMR (100 MHz,** 169.16, 160.63, 160.26, 156.69, 137.21, 135.26, 133.97,

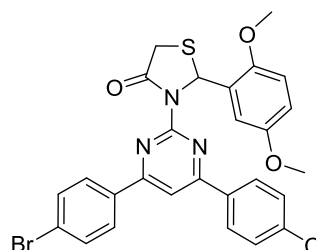
**CDCl<sub>3</sub>)** 133.51, 132.48, 131.55, 130.36, 129.82, 129.77, 129.67, 129.49, 128.79, 128.09, 122.82, 107.59, 58.52, 33.82

4.2.3.5. 3-(4-(4-bromophenyl)-6-(4-chlorophenyl)pyrimidin-2-yl)-2-(2,5-dimethoxyphenyl)thiazolidin-4-one (8e)

Yield, 40.8 %

Molecular Weight, 582.90

Molecular Formula, C<sub>27</sub>H<sub>21</sub>BrClN<sub>3</sub>O<sub>3</sub>S



**Procedure:** In 8 ml toluene and catalytic amount of glacial acetic acid, intermediate 5 (0.001 mol), was treated with 2,5-dimethoxybenzaldehyde (1 eq.), as per the procedure given in section 3.2.2.3, to yield desired product **8e**. Column chromatography (Silica gel # 60-120; Hexane:Ethyl acetate : : 80: 20) was performed to afford pure compound.

**State & colour:** Yellow solid

**R<sub>f</sub> value:** 0.42

**Melting Point:** 190-192°C

**MS (+ESI) m/z:** 606.12 [M+Na]<sup>+</sup>,  
608.11 [M+2+Na]<sup>+</sup>

**IR (cm<sup>-1</sup>)** 1712 (C=O), 1648 (C=N)

**<sup>1</sup>H NMR (400 MHz, CDCl<sub>3</sub>)** 8.21 (s, 1H), 7.93–7.91 (m, 2 H), 7.82–7.80 (m, 2 H), 7.60– 7.58 (m, 2 H), 7.35–7.33 (m, 2 H), 6.96 (s, 1H), 6.86–6.85 (m, 1H), 6.78–6.76 (m, 1H), 3.92–3.83 (m, 5 H), 3.78 (s, 3 H)

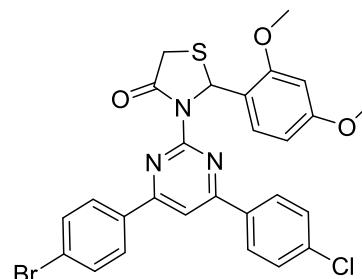
**<sup>13</sup>C NMR (100 MHz, CDCl<sub>3</sub>)** 169.17, 160.63, 160.25, 156.82, 153.82, 151.82, 135.26, 133.97, 133.51, 131.55, 129.77, 129.49, 128.79, 128.16, 122.82, 115.45, 114.49, 113.39, 107.59, 56.99, 55.62, 33.82

4.2.3.6. 3-(4-(4-bromophenyl)-6-(4-chlorophenyl)pyrimidin-2-yl)-2-(2,4-dimethoxyphenyl)thiazolidin-4-one (8f)

Yield, 35.8 %

Molecular Weight, 582.90

Molecular Formula, C<sub>27</sub>H<sub>21</sub>BrClN<sub>3</sub>O<sub>3</sub>S



**Procedure:** In 8 ml toluene and catalytic amount of glacial acetic acid, intermediate 5 (0.001 mol), was treated with 2,4-dimethoxybenzaldehyde (1 eq.), as per the procedure given in section 3.2.2.3, to yield desired product **8f**. Column chromatography (Silica gel # 60-120; Hexane:Ethyl acetate : : 80: 20) was performed to afford pure compound.

**State & colour:** Yellow solid

**R<sub>f</sub> value:** 0.42

**Melting Point:** 191-193°C

**MS (+ESI) m/z:** 606.12 [M+Na]<sup>+</sup>,  
608.11 [M+2+Na]<sup>+</sup>

**IR (cm<sup>-1</sup>)** 1716 (C=O), 1638 (C=N), 1571 (C=N), 1533 (C=N)

**<sup>1</sup>H NMR (400 MHz,** 8.21 (s, 1H), 7.93–7.91 (m, 2 H), 7.82–7.80 (m, 2 H),

**CDCl<sub>3</sub>)** 7.60–7.58 (m, 2 H), 7.35–7.33 (m, 2 H), 7.30–7.28 (m, 2 H), 6.62–6.60 (m, 1H), 6.46 (s, 1H), 3.92–3.81 (m, 8 H)

**<sup>13</sup>C NMR (100 MHz,** 169.17, 160.63, 160.33, 160.25, 158.69, 156.84, 135.26,

**CDCl<sub>3</sub>)** 133.97, 133.51, 131.55, 130.13, 129.77, 129.49, 128.79, 123.47, 122.82, 109.66, 107.59, 100.09, 56.42, 55.83, 55.66, 33.82

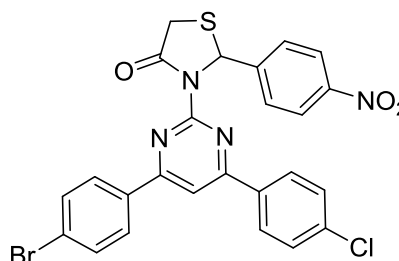


4.2.3.7. 3-(4-(4-bromophenyl)-6-(4-chlorophenyl)pyrimidin-2-yl)-2-(4-nitrophenyl)thiazolidin-4-one (**8g**)

Yield, 40.6 %

Molecular Weight, 567.84

Molecular Formula, C<sub>25</sub>H<sub>16</sub>BrClN<sub>4</sub>O<sub>3</sub>S



**Procedure:** In 8 ml toluene and catalytic amount of glacial acetic acid, intermediate 5 (0.001 mol), was treated with 4-nitrobenzaldehyde (1 eq.), as per the procedure given in section 3.2.2.3, to yield desired product **8g**. Additionally, column chromatography (Silica gel # 60-120; Hexane:Ethyl acetate : : 80: 20) was performed to afford pure compound.

**State & colour:** Yellow solid

**R<sub>f</sub> value:** 0.43

**Melting Point:** 203-205°C

**MS (+ESI) m/z:** 566.99 [M+H]<sup>+</sup>,  
568.99 [M+2+H]<sup>+</sup>

**IR (cm<sup>-1</sup>)** 1702 (C=O), 1661 (C=N), 1579 (C=N), 1536 (C=N)

**<sup>1</sup>H NMR (400 MHz, CDCl<sub>3</sub>)** 8.21–8.14 (m, 3 H), 7.93–7.91 (d, J = 8 Hz, 2 H), 7.82–7.80 (d, J = 8 Hz, 2 H), 7.61–7.58 (m, 4 H), 7.35–7.33 (d, J = 8 Hz, 2 H), 3.90–3.81 (m, 2 H)

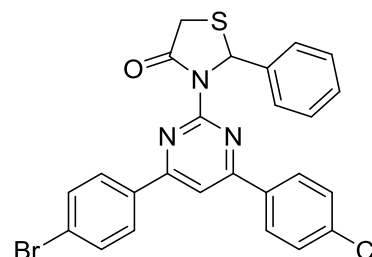
**<sup>13</sup>C NMR (100 MHz, CDCl<sub>3</sub>)** 169.01, 160.63, 160.26, 157.04, 147.49, 142.48, 135.26, 133.97, 133.51, 131.55, 129.77, 129.49, 129.01, 128.79, 124.22, 122.82, 107.59, 63.31, 33.91

**4.2.3.8. 3-(4-(4-bromophenyl)-6-(4-chlorophenyl)pyrimidin-2-yl)-2-phenylthiazolidin-4-one (8h)**

**Yield,** 20.2 %

**Molecular Weight,** 522.85

**Molecular Formula,** C<sub>25</sub>H<sub>17</sub>BrClN<sub>3</sub>OS



**Procedure:** In 8 ml toluene and catalytic amount of glacial acetic acid, intermediate 5 (0.001 mol), was treated with benzaldehyde (1 eq.), as per the procedure given in section 3.2.2.3, to yield desired product **8h**. Additionally, column chromatography (Silica gel # 60-120; Hexane:Ethyl acetate : : 80: 20) was performed to afford pure compound.

**State & colour:** Light yellow solid

**R<sub>f</sub> value:** 0.40

**Melting Point:** 180-182°C

**MS (+ESI) m/z:** 546.08 [M+Na]<sup>+</sup>,  
548.07 [M+2+Na]<sup>+</sup>

**IR (cm<sup>-1</sup>)**

1705 (C=O), 1651 (C=N), 1563 (C=N)

**<sup>1</sup>H NMR (400 MHz,**

8.21 (s, 1H), 7.93–7.91 (d, J = 8 Hz, 2 H), 7.82–7.80 (d, J

**CDCl<sub>3</sub>)**

= 8 Hz, 2 H), 7.60–7.58 (m, 2 H), 7.48–7.33 (m, 7 H),

3.90–3.81 (m, 2 H)

**<sup>13</sup>C NMR (100 MHz,**

168.99, 160.63, 160.26, 157.10, 138.81, 135.26, 133.97,

**CDCl<sub>3</sub>)**

133.51, 131.55, 129.77, 129.49, 129.21, 128.79, 128.14,

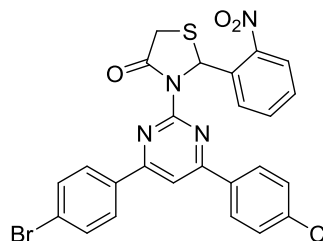
127.55, 122.82, 107.59

4.2.3.9. 3-(4-(4-bromophenyl)-6-(4-chlorophenyl)pyrimidin-2-yl)-2-(2-nitrophenyl)thiazolidin-4-one (**8i**)

Yield, 24.5 %

Molecular Weight, 567.84

Molecular Formula, C<sub>25</sub>H<sub>16</sub>BrClN<sub>4</sub>O<sub>3</sub>S



**Procedure:** In 8 ml toluene and catalytic amount of glacial acetic acid, intermediate 5 (0.001 mol), was treated with 2-nitrobenzaldehyde (1 eq.), as per the procedure given in section 3.2.2.3, to yield desired product **8i**. Additionally, column chromatography (Silica gel # 60-120; Hexane:Ethyl acetate : : 80: 20) was performed to afford pure compound.

**State & colour:** Light yellow solid

**R<sub>f</sub> value:** 0.44

**Melting Point:** 206-208°C

**MS (+ESI) m/z:** 566.99 [M+H]<sup>+</sup>,  
568.99 [M+2+H]<sup>+</sup>

**IR (cm<sup>-1</sup>)** 1708 (C=O), 1662 (C=N), 1586 (C=N), 1534 (C=N)

**<sup>1</sup>H NMR (400 MHz, CDCl<sub>3</sub>)** 8.21 (s, 1H), 7.97–7.91 (m, 3 H), 7.82–7.80 (m, 3 H),  
7.61–7.50 (m, 4 H), 7.35–7.33 (m, 2 H), 3.92–3.83 (m, 2 H)

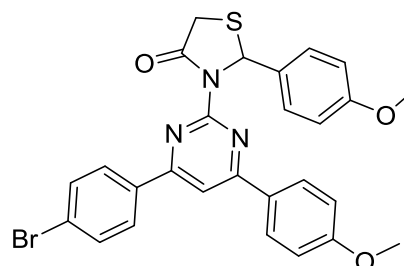
**<sup>13</sup>C NMR (100 MHz, CDCl<sub>3</sub>)** 169.20, 160.63, 160.25, 157.02, 148.07, 135.26, 134.63,  
133.97, 133.51, 132.93, 131.55, 129.77, 129.49, 129.37,  
128.79, 128.70, 125.01, 122.82, 107.59, 57.03, 33.87

4.2.3.10. 3-(4-(4-bromophenyl)-6-(4-methoxyphenyl)pyrimidin-2-yl)-2-(4-methoxyphenyl)thiazolidin-4-one (**8j**)

Yield, 30.5 %

Molecular Weight, 548.46

Molecular Formula, C<sub>27</sub>H<sub>22</sub>BrN<sub>3</sub>O<sub>3</sub>S



**Procedure:** In 8 ml toluene and catalytic amount of glacial acetic acid, intermediate 5 (0.001 mol), was treated with 4-methoxybenzaldehyde (1 eq.), as per the procedure given in section 3.2.2.3, to yield desired product **8j**. Additionally, column chromatography (Silica gel # 60-120; Hexane:Ethyl acetate : : 80: 20) was performed to afford pure compound.

**State & colour:** Yellow solid

**R<sub>f</sub> value:** 0.39

**Melting Point:** 186-188°C

**MS (+ESI) m/z:** 552.02 [M+H]<sup>+</sup>,  
554.01 [M+2+H]<sup>+</sup>

**IR (cm<sup>-1</sup>)** 1715 (C=O), 1674 (C=N), 1580 (C=N), 1522 (C=N)

**<sup>1</sup>H NMR (400 MHz, CDCl<sub>3</sub>)** 8.35 (s, 1H) 7.82–7.79 (m, 4 H), 7.60– 7.58 (m, 2 H),  
7.22–7.20 (m, 2 H), 6.90–6.85 (m, 4 H), 3.90–3.80 (m, 8 H)

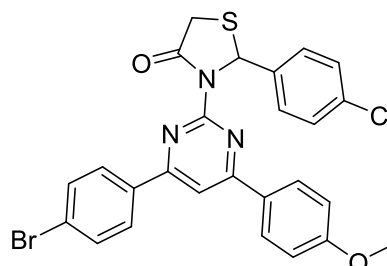
**<sup>13</sup>C NMR (100 MHz, CDCl<sub>3</sub>)** 168.99, 160.25, 160.22, 159.51, 159.41, 157.04, 133.97,  
133.55, 131.55, 129.76, 129.58, 129.49, 128.87, 122.82,  
114.29, 114.18, 107.50, 63.29, 55.37, 55.35, 33.91

4.2.3.11. 3-(4-(4-bromophenyl)-6-(4-methoxyphenyl)pyrimidin-2-yl)-2-(4-chlorophenyl)thiazolidin-4-one (**8k**)

Yield, 22.5 %

Molecular Weight, 552.87

Molecular Formula, C<sub>26</sub>H<sub>19</sub>BrClN<sub>3</sub>O<sub>2</sub>S



**Procedure:** In 8 ml toluene and catalytic amount of glacial acetic acid, intermediate **5** (0.001 mol), was treated with 4-chlorobenzaldehyde (1 eq.), as per the procedure given in section 3.2.2.3, to yield desired product **8k**. Additionally, column chromatography (Silica gel # 60-120; Hexane:Ethyl acetate : : 80: 20) was performed to afford pure compound.

**State & colour:** Yellow solid

**R<sub>f</sub> value:** 0.36

**Melting Point:** 196-198°C

**MS (+ESI) m/z:** 554.01 [M+H]<sup>+</sup>,  
556.01 [M+2+H]<sup>+</sup>

**IR (cm<sup>-1</sup>)** 1722 (C=O), 1652 (C=N), 1573 (C=N), 1554 (C=N)

**<sup>1</sup>H NMR (400 MHz,** 8.19 (s, 1H) 7.82–7.79 (m, 4 H), 7.60–7.58 (m, 2 H),

**CDCl<sub>3</sub>)** 7.30 (m, 4 H), 6.90–6.88 (m, 2 H), 3.90–3.80 (m, 5 H)

**<sup>13</sup>C NMR (100 MHz,** 168.99, 160.25, 160.22, 159.41, 157.04, 136.91, 134.36,

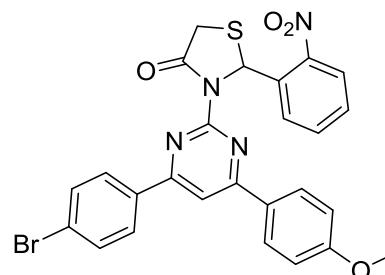
**CDCl<sub>3</sub>)** 133.97, 131.55, 129.76, 129.58, 129.49, 129.31, 129.28,  
122.82, 114.18, 107.50, 63.03, 55.35, 33.91

4.2.3.12. 3-(4-(4-bromophenyl)-6-(4-methoxyphenyl)pyrimidin-2-yl)-2-(2-nitrophenyl) thiazolidin-4-one (8l)

Yield, 32.5 %

Molecular Weight, 563.43

Molecular Formula, C<sub>26</sub>H<sub>19</sub>BrN<sub>4</sub>O<sub>4</sub>S



**Procedure:** In 8 ml toluene and catalytic amount of glacial acetic acid, intermediate 5 (0.001 mol), was treated with 2-nitrobenzaldehyde (1 eq.), as per the procedure given in section 3.2.2.3, to yield desired product **8l**. Additionally, column chromatography (Silica gel # 60-120; Hexane:Ethyl acetate : : 80: 20) was performed to afford pure compound.

**State & colour:** Yellow solid

**R<sub>f</sub> value:** 0.38

**Melting Point:** 188-190°C

**MS (+ESI) m/z:** 563.04 [M+H]<sup>+</sup>,  
565.04 [M+2+H]<sup>+</sup>

**IR (cm<sup>-1</sup>)**

1723 (C=O), 1654 (C=N), 1570 (C=N), 1524 (C=N)

**<sup>1</sup>H NMR (400 MHz,**

8.19 (s, 1H) 7.97–7.95 (m, 1H), 7.82–7.79 (m, 4 H),

CDCl<sub>3</sub>)

7.60–7.51 (m, 5 H), 6.90–6.88 (m, 2 H), 3.91–3.80 (m, 2 H)

**<sup>13</sup>C NMR (100 MHz,**

169.20, 160.26, 160.25, 159.41, 157.08, 148.07, 134.63,

CDCl<sub>3</sub>)

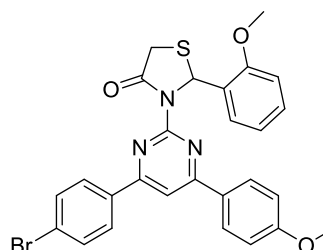
133.97, 132.93, 131.55, 129.76, 129.58, 129.49, 129.37,  
128.70, 125.01, 122.82, 114.18, 107.50, 57.03, 55.35,  
33.87

4.2.3.13. 3-(4-(4-bromophenyl)-6-(4-methoxyphenyl)pyrimidin-2-yl)-2-(2-methoxyphenyl) thiazolidin-4-one (**8m**)

Yield, 32.5 %

Molecular Weight, 548.46

Molecular Formula, C<sub>27</sub>H<sub>22</sub>BrN<sub>3</sub>O<sub>3</sub>S



**Procedure:** In 8 ml toluene and catalytic amount of glacial acetic acid, intermediate 5 (0.001 mol), was treated with 2-methoxybenzaldehyde (1 eq.), as per the procedure given in section 3.2.2.3, to yield desired product **8m**. Additionally, column chromatography (Silica gel # 60-120; Hexane:Ethyl acetate : : 80: 20) was performed to afford pure compound.

**State & colour:** Yellow solid

**R<sub>f</sub> value:** 0.38

**Melting Point:** 188-190°C

**MS (+ESI) m/z:** 550.04 [M+H]<sup>+</sup>,  
552.04 [M+2+H]<sup>+</sup>

**IR (cm<sup>-1</sup>)** 1723 (C=O), 1654 (C=N), 1570 (C=N), 1524 (C=N)

**<sup>1</sup>H NMR (400 MHz, CDCl<sub>3</sub>)** 8.19 (s, 1H), 7.82-7.79 (m, 4H), 7.60-7.58 (m, 2H), 7.48-7.46 (m, 1H), 7.24-7.20 (m, 1H), 7.14-7.11 (m, 2H), 6.96-6.94 (m, 1H), 6.90-6.88 (m, 2H), 3.92-3.80 (m, 8H)

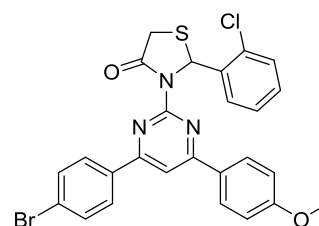
**<sup>13</sup>C NMR (100 MHz, CDCl<sub>3</sub>)** 169.17, 160.25, 160.22, 159.41, 157.51, 156.86, 133.97, 131.55, 129.76, 129.58, 129.49, 129.35, 128.75, 126.63, 122.82, 122.38, 114.18, 112.76, 107.50, 56.45, 55.62, 55.35, 33.82

4.2.3.14. 3-(4-(4-bromophenyl)-6-(4-methoxyphenyl)pyrimidin-2-yl)-2-(2-chlorophenyl)thiazolidin-4-one (**8n**)

Yield, 32.5 %

Molecular Weight, 552.87

Molecular Formula, C<sub>26</sub>H<sub>19</sub>BrClN<sub>3</sub>O<sub>2</sub>S



**Procedure:** In 8 ml toluene and catalytic amount of glacial acetic acid, intermediate 5 (0.001 mol), was treated with 2-chlorobenzaldehyde (1 eq.), as per the procedure given in section 3.2.2.3, to yield desired product **8n**. Additionally, column chromatography (Silica gel # 60-120; Hexane:Ethyl acetate : : 80: 20) was performed to afford pure compound.

**State & colour:** Light yellow solid

**R<sub>f</sub> value:** 0.38

**Melting Point:** 188-190°C

**MS (+ESI) m/z:** 554.04 [M+H]<sup>+</sup>,  
556.04 [M+2+H]<sup>+</sup>

**IR (cm<sup>-1</sup>)** 1723 (C=O), 1654 (C=N), 1570 (C=N), 1524 (C=N)

**<sup>1</sup>H NMR (400 MHz, CDCl<sub>3</sub>)** 8.19 (s, 1H), 7.82-7.79 (m, 4H), 7.60-7.58 (m, 2H), 7.45-7.27 (m, 4H), 6.90-6.88 (m, 2H), 3.92-3.80 (m, 5H)

**<sup>13</sup>C NMR (100 MHz, CDCl<sub>3</sub>)** 169.16, 160.25, 160.22, 159.41, 156.69, 137.21, 133.97, 132.48, 131.55, 130.36, 129.82, 129.76, 129.67, 129.58, 129.49, 128.09, 122.82, 114.18, 107.50, 58.52, 55.35, 33.82

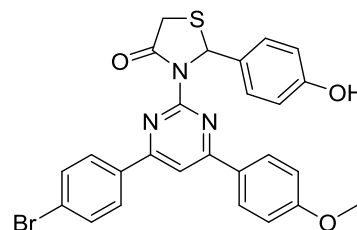


**4.2.3.15. 3-(4-(4-bromophenyl)-6-(4-methoxyphenyl)pyrimidin-2-yl)-2-(4-hydroxyphenyl)thiazolidin-4-one (8o)**

**Yield,** 32.5 %

**Molecular Weight,** 534.43

**Molecular Formula,** C<sub>26</sub>H<sub>20</sub>BrN<sub>3</sub>O<sub>3</sub>S



**Procedure:** In 8 ml toluene and catalytic amount of glacial acetic acid, intermediate 5 (0.001 mol), was treated with 4-hydroxybenzaldehyde (1 eq.), as per the procedure given in section 3.2.2.3, to yield desired product **8o**. Additionally, column chromatography (Silica gel # 60-120; Hexane:Ethyl acetate : : 80: 20) was performed to afford pure compound.

**State & colour:** Light yellow solid

**R<sub>f</sub> value:** 0.38

**Melting Point:** 188-190°C

**MS (+ESI) m/z:** 535.04 [M+H]<sup>+</sup>,  
537.04 [M+2+H]<sup>+</sup>

**IR (cm<sup>-1</sup>)** 1723 (C=O), 1654 (C=N), 1570 (C=N), 1524 (C=N)

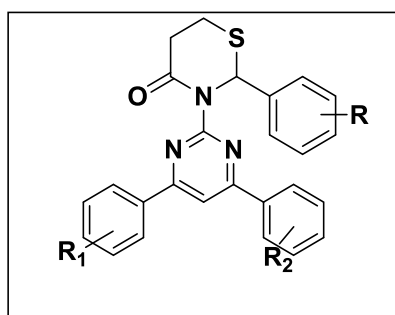
**<sup>1</sup>H NMR (400 MHz, CDCl<sub>3</sub>)** 8.19-8.16 (m, 2H) 7.82-7.79 (m, 4H), 7.60-7.58 (m, 2H),  
7.19-7.16 (m, 2H), 7.08 (s, 1H), 6.90-6.88 (m, 2H), 6.80-  
6.78 (m, 2H), 3.92-3.80 (m, 5H)

**<sup>13</sup>C NMR (100 MHz, DCl<sub>3</sub>)** 168.99, 160.25, 160.22, 159.41, 157.93, 157.04, 133.97,  
132.16, 131.55, 129.76, 129.58, 129.49, 129.39, 122.82,  
116.10, 114.18, 107.50, 63.39, 55.35, 33.91

**4.2.4. Characterization of compounds pertaining to Formula-II (10a-10o)**

After the synthesis of designed compounds, characterization of the compounds was done *via* <sup>1</sup>H-NMR, <sup>13</sup>C NMR and Mass spectrometry. The peaks in spectral analysis

were assigned to structural features of synthesized compounds using various literature sources (Silverstein and Bassler 1962; Kemp 1991; Pavia, Lampman et al. 2014). The physical properties of the compounds pertaining to formula-II have been given in **Table 4.16**. In general, the IR spectrum for the 1,3-thiazin-4-one-pyrimidine derivatives exhibited a characteristic absorption band for C=O of amide from  $\sim 1680$  to  $\sim 1695$   $\text{cm}^{-1}$  and absorption bands for aromatic C=N from  $\sim 1690$  to  $\sim 1550$   $\text{cm}^{-1}$  were also observed. The  $^1\text{H-NMR}$  spectrum for all the 1,3-thiazin-4-one-pyrimidine derivatives showed characteristic singlet around  $\sim 8.2$  ppm for one proton presents in the pyrimidine nucleus; the value deviated slightly in different derivatives because of the electronic nature of the substituents. Most of the aromatic protons retained their pattern throughout the series and appeared at similar values from  $\sim 6.7$  to  $\sim 7.9$  ppm. For both the neighboring methylene ( $-\text{CH}_2$ ), overlapped doublets, appearing as multiplet of two protons each, were observed between  $\sim 2.8$  to  $\sim 3.3$  ppm which confirmed the formation of the 1,3-thiazin-4-one ring. Accordingly, mass spectra also showed the presence of the expected fragmentation pattern with quasi-ion peaks at the required  $m/z$  values. Characteristic  $M + 2$  and  $M + 4$  values were also recorded in each mass spectrum due to presence of halogen atoms throughout the series.

**Formula-II**

**Table 4.16.** Physical characteristics of synthesized compounds pertaining to Formula-II (10a-10o).

Comp. Code	R	R <sub>1</sub>	R <sub>2</sub>	Color	R <sub>f</sub> value <sup>a</sup> Hexane: EtAc	% Yield	Melting point <sup>b</sup> (°C)
10a	4-Cl	Br	Cl	Light yellow	0.33	32%	207–209
10b	2-Cl	Br	Cl	Light yellow	0.37	36%	205–207
10c	2-OCH <sub>3</sub>	Br	Cl	Light yellow	0.39	32.1%	190–192
10d	4-OH	Br	Cl	Light yellow	0.35	40%	212–214
10e	2,5-di-OCH <sub>3</sub>	Br	Cl	Yellow	0.43	38%	185–187
10f	2,4-di-OCH <sub>3</sub>	Br	Cl	Yellow	0.43	38%	186–188
10g	4-NO <sub>2</sub>	Br	Cl	Yellow	0.44	36%	198–200
10h	H	Br	Cl	Yellow	0.41	22%	179–181
10i	2-NO <sub>2</sub>	Br	Cl	Light yellow	0.45	24%	201–203
10j	4-OCH <sub>3</sub>	Br	OCH <sub>3</sub>	Yellow	0.40	35%	181–183
10k	4-Cl	Br	OCH <sub>3</sub>	Light Yellow	0.37	25%	191–193
10l	2-NO <sub>2</sub>	Br	OCH <sub>3</sub>	Light yellow	0.41	31%	183–185
10m	2-OCH <sub>3</sub>	Br	OCH <sub>3</sub>	Light	0.37	29%	183–185

				yellow				
<b>10n</b>	2-Cl	Br	OCH <sub>3</sub>	Light	0.37	27%	194-196	
				yellow				
<b>10o</b>	4-OH	Br	OCH <sub>3</sub>	Light	0.38	36%	187-189	
				yellow				

<sup>a</sup>EtAc: ethyl acetate

<sup>b</sup>Determined melting points are uncorrected.

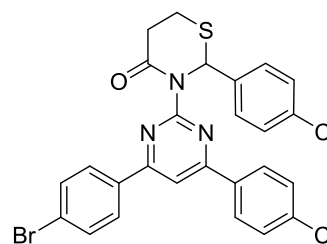
#### 4.2.5. Compound sheets

##### 4.2.5.1. 3-(4-(4-bromophenyl)-6-(4-chlorophenyl)pyrimidin-2-yl)-2-(4-chlorophenyl)-1,3-thiazinan-4-one (10a)

**Yield,** 32 %

**Molecular Weight,** 571.31

**Molecular Formula,** C<sub>26</sub>H<sub>18</sub>BrCl<sub>2</sub>N<sub>3</sub>OS



**Procedure:** The intermediate 5 (0.001 mol) was treated with 4-chlorobenzaldehyde (1 eq.), dissolved in toluene and catalytic amount of glacial acetic acid, as per the procedure given in section 3.2.3.1, to yield desired product **10a**. Column chromatography (Silica gel # 60-120; Hexane:Ethyl acetate : : 80: 20) was performed to afford pure compound.

**State & colour:** Light yellow solid

**R<sub>f</sub> value:** 0.33

**Melting Point:** 207-209°C

**MS (+ESI) m/z:** 571.97 [M+H]<sup>+</sup>,  
573.96 [M+2+H]<sup>+</sup>

**IR (cm<sup>-1</sup>)** 1717 (C=O), 1659 (C=N), 1630 (C=N), 1589 (C=N)

**<sup>1</sup>H NMR (400 MHz,** 8.21 (s, 1H), 7.93-7.91 (m, 2H), 7.82-7.80 (m, 2H), 7.60-

**CDCl<sub>3</sub>)** 7.58 (m, 2H), 7.35-7.29 (m, 6H), 6.45 (m, 1H), 3.04-3.02

(m, 2H), 2.90-2.88 (m, 2H)

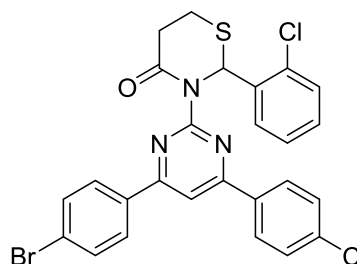
$^{13}\text{C}$ NMR (100 MHz, $\text{CDCl}_3$ )	166.82, 160.49, 160.17, 156.93, 136.44, 135.26, 134.38, 133.97, 133.51, 131.55, 129.77, 129.49, 129.36, 129.28, 128.79, 122.82, 107.48, 62.80, 34.20, 26.64
---	---

#### 4.2.5.2. 3-(4-(4-bromophenyl)-6-(4-chlorophenyl)pyrimidin-2-yl)-2-(2-chlorophenyl)-1,3-thiazinan-4-one (10b)

Yield, 32 %

Molecular Weight, 571.31

Molecular Formula,  $\text{C}_{26}\text{H}_{18}\text{BrCl}_2\text{N}_3\text{OS}$



**Procedure:** The intermediate 5 (0.001 mol) was treated with 2-chlorobenzaldehyde (1 eq.), dissolved in toluene and catalytic amount of glacial acetic acid, as per the procedure given in section 3.2.3.1, to yield desired product **10b**. Additionally, column chromatography (Silica gel # 60-120; Hexane:Ethyl acetate : : 80: 20) was performed to afford pure compound.

**State & colour:** Light yellow solid

**R<sub>f</sub> value:** 0.37

**Melting Point:** 205-207°C

**MS (+ESI) m/z:** 571.97  $[\text{M}+\text{H}]^+$ ,  
573.96  $[\text{M}+2+\text{H}]^+$

**IR (cm<sup>-1</sup>)** 1721 (C=O), 1635 (C=N), 1611 (C=N), 1572 (C=N)

**$^1\text{H}$  NMR (400 MHz,  $\text{CDCl}_3$ )** 8.21 (s, 1H), 7.93-7.91 (m, 2H), 7.82-7.80 (m, 2H), 7.60-7.58 (m, 2H), 7.45-7.27 (m, 6H), 6.86 (m, 1H), 3.07-3.05 (m, 2H), 2.90-2.88 (m, 2H)

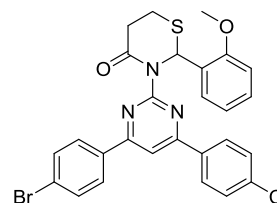
**$^{13}\text{C}$  NMR (100 MHz,  $\text{CDCl}_3$ )** 166.83, 160.49, 160.17, 156.68, 135.96, 135.26, 133.97, 133.51, 132.84, 131.55, 130.33, 129.90, 129.77, 129.70, 129.49, 128.79, 128.04, 122.82, 107.48, 57.94, 34.20, 26.65

4.2.5.3. **3-(4-(4-bromophenyl)-6-(4-chlorophenyl)pyrimidin-2-yl)-2-(2-methoxyphenyl)-1,3-thiazinan-4-one (10c)**

**Yield,** 31 %

**Molecular Weight,** 566.90

**Molecular Formula,** C<sub>27</sub>H<sub>21</sub>BrClN<sub>3</sub>O<sub>2</sub>S



**Procedure:** The intermediate 5 (0.001 mol) was treated with 2-methoxybenzaldehyde (1 eq.), dissolved in toluene and catalytic amount of glacial acetic acid, as per the procedure given in section 3.2.3.1, to yield desired product **10c**. Column chromatography (Silica gel # 60-120; Hexane:Ethyl acetate : : 80: 20) was performed to afford pure compound.

**State & colour:** Light yellow solid

**R<sub>f</sub> value:** 0.39

**Melting Point:** 190-192°C

**MS (+ESI) m/z:** 567.02 [M+H]<sup>+</sup>,  
569.01 [M+2+H]<sup>+</sup>

**IR (cm<sup>-1</sup>)** 1721 (C=O), 1635 (C=N), 1611 (C=N), 1572 (C=N)

**<sup>1</sup>H NMR (400 MHz, CDCl<sub>3</sub>)** 8.21 (s, 1H), 7.93-7.91 (m, 2H), 7.82-7.80 (m, 2H), 7.60-7.58 (m, 2H), 7.48-7.46 (m, 1H), 7.35-7.33 (m, 2H), 7.22-7.20 (m, 1H), 7.14-7.13 (m, 1H), 6.96-6.94 (m, 1H), 6.85 (m, 1H), 3.84 (s, 3H), 3.07-3.04 (m, 2H), 2.90-2.88 (m, 2H)

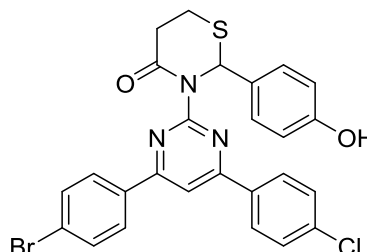
**<sup>13</sup>C NMR (100 MHz, CDCl<sub>3</sub>)** 166.85, 160.49, 160.17, 157.35, 156.94, 135.26, 133.97, 133.51, 131.55, 129.77, 129.49, 129.40, 128.79, 128.78, 124.06, 122.82, 122.33, 112.75, 107.48, 58.35, 55.62, 34.20, 26.62

4.2.5.4. 3-(4-(4-bromophenyl)-6-(4-chlorophenyl)pyrimidin-2-yl)-2-(4-hydroxyphenyl)-1,3-thiazinan-4-one (10d)

Yield, 40 %

Molecular Weight, 552.87

Molecular Formula, C<sub>26</sub>H<sub>19</sub>BrClN<sub>3</sub>O<sub>2</sub>S



**Procedure:** The intermediate 5 (0.001 mol) was treated with 4-hydroxybenzaldehyde (1 eq.), dissolved in toluene and catalytic amount of glacial acetic acid, as per the procedure given in section 3.2.3.1, to yield desired product **10d**. Column chromatography (Silica gel # 60-120; Hexane:Ethyl acetate : : 80: 20) was performed to afford pure compound.

**State & colour:** Light yellow solid

**R<sub>f</sub> value:** 0.35

**Melting Point:** 212-214°C

**MS (+ESI) m/z:** 554.54 [M+H]<sup>+</sup>,  
556.51 [M+2+H]<sup>+</sup>

**IR (cm<sup>-1</sup>)** 1714 (C=O), 1644 (C=N), 1574 (C=N)

**<sup>1</sup>H NMR (400 MHz, CDCl<sub>3</sub>)** 8.21 (s, 1H), 8.16 (s, 1H), 7.93-7.91 (m, 2H), 7.82-7.80 (m, 2H), 7.60-7.58 (m, 2H), 7.35-7.33 (m, 2H), 7.19-7.17 (m, 2H), 6.80-6.78 (m, 2H), 6.44 (s, 1H), 3.04-3.02 (m, 2H), 2.90-2.88 (m, 2H)

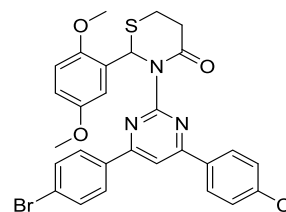
**<sup>13</sup>C NMR (100 MHz, CDCl<sub>3</sub>)** 166.82, 160.49, 160.17, 157.92, 156.93, 135.26, 133.97, 133.51, 131.55, 130.08, 129.77, 129.55, 129.49, 128.79, 122.82, 116.09, 107.48, 63.22, 34.20, 26.64

4.2.5.5. **3-(4-(4-bromophenyl)-6-(4-chlorophenyl)pyrimidin-2-yl)-2-(2,5-dimethoxyphenyl)-1,3-thiazinan-4-one (10e)**

**Yield,** 38 %

**Molecular Weight,** 596.92

**Molecular Formula,** C<sub>28</sub>H<sub>23</sub>BrClN<sub>3</sub>O<sub>3</sub>S



**Procedure:** The intermediate 5 (0.001 mol) was treated with 2, 5-dimethoxybenzaldehyde (1 eq.), dissolved in toluene and catalytic amount of glacial acetic acid, as per the procedure given in section 3.2.3.1, to yield desired product **10e**. Column chromatography (Silica gel # 60-120; Hexane:Ethyl acetate : : 80: 20) was performed to afford pure compound.

**State & colour:** Light yellow solid

**R<sub>f</sub> value:** 0.43

**Melting Point:** 185-187°C

**MS (+ESI) m/z:** 597.12 [M+H]<sup>+</sup>,  
599.11 [M+2+H]<sup>+</sup>

**IR (cm<sup>-1</sup>)** 1712 (C=O), 1648 (C=N)

**<sup>1</sup>H NMR (400 MHz, CDCl<sub>3</sub>)** 8.21 (s, 1H), 7.93-7.91 (m, 2H), 7.82-7.80 (m, 2H), 7.60-7.58 (m, 2H), 7.35-7.33 (m, 2H), 7.05 (m, 1H), 6.89-6.88 (m, 1H), 6.84 (m, 1H), 6.80-6.78 (m, 1H), 3.84 (s, 3H), 3.78 (s, 3H), 3.07-3.04 (m, 2H), 2.90-2.88 (m, 2H)

**<sup>13</sup>C NMR (100 MHz, CDCl<sub>3</sub>)** 166.81, 160.49, 160.17, 156.92, 153.83, 151.49, 135.26, 133.97, 133.51, 131.55, 129.77, 129.49, 129.14, 128.79, 122.82, 115.35, 114.51, 113.36, 107.48, 58.76, 55.62, 34.20, 26.62

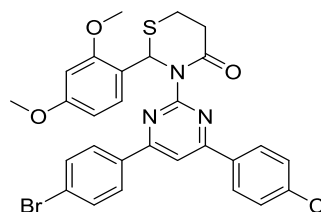


4.2.5.6. 3-(4-(4-bromophenyl)-6-(4-chlorophenyl)pyrimidin-2-yl)-2-(2,4-dimethoxyphenyl)-1,3-thiazinan-4-one (10f)

Yield, 38 %

Molecular Weight, 596.92

Molecular Formula, C<sub>28</sub>H<sub>23</sub>BrClN<sub>3</sub>O<sub>3</sub>S



**Procedure:** The intermediate 5 (0.001 mol) was treated with 2, 4-dimethoxybenzaldehyde (1 eq.), dissolved in toluene and catalytic amount of glacial acetic acid, as per the procedure given in section 3.2.3.1, to yield desired product **10f**. Column chromatography (Silica gel # 60-120; Hexane:Ethyl acetate : : 80: 20) was performed to afford pure compound.

**State & colour:** Yellow solid

**R<sub>f</sub> value:** 0.43

**Melting Point:** 186-188°C

**MS (+ESI) m/z:** 598.12 [M+H]<sup>+</sup>,  
600.11 [M+2+H]<sup>+</sup>

**IR (cm<sup>-1</sup>)** 1716 (C=O), 1638 (C=N), 1571 (C=N), 1533 (C=N)

**<sup>1</sup>H NMR (400 MHz, CDCl<sub>3</sub>)** 8.21 (s, 1H), 7.93-7.91 (m, 2H), 7.82-7.80 (m, 2H), 7.60-7.58 (m, 2H), 7.37-7.33 (m, 3H), 6.91 (m, 1H), 6.63-6.61 (m, 1H), 6.51 (m, 1H), 3.83-3.81 (m, 6H), 3.07-3.04 (m, 2H), 2.90-2.88 (m, 2H)

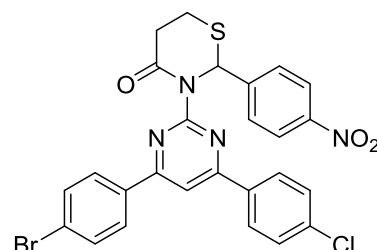
**<sup>13</sup>C NMR (100 MHz, CDCl<sub>3</sub>)** 166.86, 160.49, 160.31, 160.17, 158.69, 156.96, 135.26, 133.97, 133.51, 131.55, 130.22, 129.77, 129.49, 128.79, 122.82, 120.79, 109.59, 107.48, 100.11, 58.31, 55.83, 55.66, 34.20, 26.62

4.2.5.7. **3-(4-(4-bromophenyl)-6-(4-chlorophenyl)pyrimidin-2-yl)-2-(4-nitrophenyl)-1,3-thiazinan-4-one (10g)**

Yield, 36 %

Molecular Weight, 581.87

Molecular Formula, C<sub>26</sub>H<sub>18</sub>BrClN<sub>4</sub>O<sub>3</sub>S



**Procedure:** The intermediate 5 (0.001 mol) was treated with 4-nitrobenzaldehyde (1 eq.), dissolved in toluene and catalytic amount of glacial acetic acid, as per the procedure given in section 3.2.3.1, to yield desired product **10g**. Column chromatography (Silica gel # 60-120; Hexane:Ethyl acetate : : 80: 20) was performed to afford pure compound.

**State & colour:** Yellow solid

**R<sub>f</sub> value:** 0.44

**Melting Point:** 198-200°C

**MS (+ESI) m/z:** 582.99 [M+H]<sup>+</sup>,  
584.99 [M+2+H]<sup>+</sup>

**IR (cm<sup>-1</sup>)** 1702 (C=O), 1661 (C=N), 1579 (C=N), 1536 (C=N)

**<sup>1</sup>H NMR (400 MHz, CDCl<sub>3</sub>)** 8.21 (s, 1H), 8.15-8.13 (m, 2H), 7.93-7.91 (m, 2H), 7.82-7.80 (m, 2H), 7.71-7.69 (m, 2H), 7.60-7.58 (m, 2H), 7.35-7.33 (m, 3H), 6.52 (m, 1H), 3.04-3.02 (m, 2H), 2.90-2.88 (m, 2H)

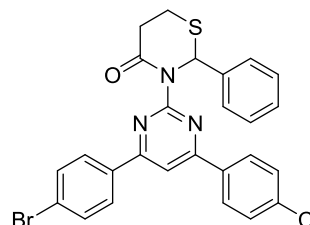
**<sup>13</sup>C NMR (100 MHz, CDCl<sub>3</sub>)** 166.82, 160.49, 160.17, 156.93, 147.53, 142.92, 135.26, 133.97, 133.51, 131.55, 129.77, 129.49, 129.20, 128.79, 124.20, 122.82, 107.48, 63.13, 34.20, 26.69

#### 4.2.5.8. 3-(4-(4-bromophenyl)-6-(4-chlorophenyl)pyrimidin-2-yl)-2-phenyl-1,3-thiazinan-4-one (10h)

Yield, 22%

Molecular Weight, 536.87

Molecular Formula, C<sub>26</sub>H<sub>19</sub>BrClN<sub>3</sub>OS



**Procedure:** The intermediate 5 (0.001 mol) was treated with benzaldehyde (1 eq.), dissolved in 8ml toluene and catalytic amount of glacial acetic acid, as per the procedure given in section 3.2.3.1, to yield desired product **10h**. Column chromatography (Silica gel # 60-120; Hexane:Ethyl acetate : : 80: 20) was performed to afford pure compound.

**State & colour:** Yellow solid

**R<sub>f</sub> value:** 0.41

**Melting Point:** 179-181°C

**MS (+ESI) m/z:** 538.08 [M+H]<sup>+</sup>,  
540.07 [M+2+H]<sup>+</sup>

**IR (cm<sup>-1</sup>)** 1705 (C=O), 1653 (C=N), 1562 (C=N)

**<sup>1</sup>H NMR (400 MHz, CDCl<sub>3</sub>)** 8.21 (s, 1H), 7.93-7.91 (m, 2H), 7.82-7.80 (m, 2H), 7.60-7.58 (m, 2H), 7.49-7.41 (m, 5H), 7.35-7.33 (m, 2H), 6.36 (s, 1H), 3.04-3.02 (m, 2H), 2.90-2.88 (m, 2H)

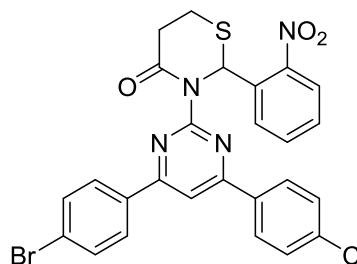
**<sup>13</sup>C NMR (100 MHz, CDCl<sub>3</sub>)** 166.83, 160.49, 160.17, 156.88, 138.04, 135.26, 133.97, 133.51, 131.55, 129.77, 129.49, 129.17, 128.79, 128.25, 127.55, 122.82, 107.48, 63.15, 34.20, 26.64

#### 4.2.5.9. 3-(4-(4-bromophenyl)-6-(4-chlorophenyl)pyrimidin-2-yl)-2-(2-nitrophenyl)-1,3-thiazinan-4-one (10i)

Yield, 24%

Molecular Weight, 581.87

Molecular Formula, C<sub>26</sub>H<sub>18</sub>BrClN<sub>4</sub>O<sub>3</sub>S



**Procedure:** The intermediate 5 (0.001 mol) was treated with 2-nitrobenzaldehyde (1 eq.), dissolved in 8ml toluene and catalytic amount of glacial acetic acid, as per the procedure given in section 3.2.3.1, to yield desired product **10i**. Column chromatography (Silica gel # 60-120; Hexane:Ethyl acetate : : 80: 20) was performed to afford pure compound.

**State & colour:** Light yellow solid

**R<sub>f</sub> value:** 0.45

**Melting Point:** 201-203°C

**MS (+ESI) m/z:** 583.99 [M+H]<sup>+</sup>,  
585.99 [M+2+H]<sup>+</sup>

**IR (cm<sup>-1</sup>)** 1708 (C=O), 1662 (C=N), 1586 (C=N), 1534 (C=N)

**<sup>1</sup>H NMR (400 MHz, CDCl<sub>3</sub>)** 8.21 (s, 1H), 7.99-7.97 (m, 1H), 7.93-7.91 (m, 2H), 7.82-7.80 (m, 2H), 7.72-7.70 (m, 1H), 7.63-7.50 (m, 4H), 7.35-7.28 (m, 3H), 3.07-3.04 (m, 2H), 2.90-2.88 (m, 2H)

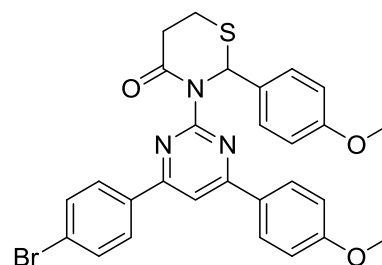
**<sup>13</sup>C NMR (100 MHz, CDCl<sub>3</sub>)** 166.70, 160.49, 160.17, 157.14, 147.93, 135.26, 134.10, 133.97, 133.51, 132.96, 131.55, 129.77, 129.49, 129.44, 128.79, 128.71, 124.98, 122.82, 107.48, 55.74, 34.20, 26.55

#### 4.2.5.10. 3-(4-(4-bromophenyl)-6-(4-methoxyphenyl)pyrimidin-2-yl)-2-(4-methoxyphenyl)-1,3-thiazinan-4-one (10j)

**Yield,** 35%

**Molecular Weight,** 562.48

**Molecular Formula,** C<sub>28</sub>H<sub>24</sub>BrN<sub>3</sub>O<sub>3</sub>S



**Procedure:** The intermediate 5 (0.001 mol) was treated with 4-methoxybenzaldehyde (1 eq.), dissolved in 8ml toluene and catalytic amount of glacial acetic acid, as per the

procedure given in section 3.2.3.1, to yield desired product **10j**. Column chromatography (Silica gel # 60-120; Hexane:Ethyl acetate : : 80: 20) was performed to afford pure compound.

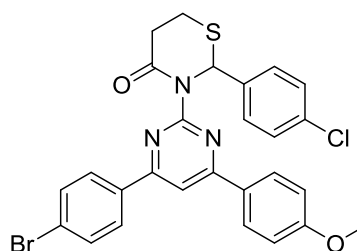
<b>State &amp; colour:</b>	Yellow solid	<b>R<sub>f</sub> value:</b>	0.40
<b>Melting Point:</b>	181-183°C	<b>MS (+ESI) m/z:</b>	563.02 [M+H] <sup>+</sup> , 565.01 [M+2+H] <sup>+</sup>
<b>IR (cm<sup>-1</sup>)</b>	1705 (C=O), 1674 (C=N), 1580 (C=N), 1522 (C=N)		
<b><sup>1</sup>H NMR (400 MHz, CDCl<sub>3</sub>)</b>	8.19 (s, 1H), 7.82-7.79 (m, 4H), 7.60-7.58 (m, 2H), 7.30-7.28 (m, 2H), 6.90-6.87 (m, 4H), 6.44 (s, 1H), 3.80 (s, 6H), 3.04-3.02 (m, 2H), 2.90-2.88 (m, 2H)		
<b><sup>13</sup>C NMR (100 MHz, CDCl<sub>3</sub>)</b>	166.82, 160.17, 160.11, 159.53, 159.41, 156.93, 133.97, 131.72, 131.55, 129.76, 129.58, 129.49, 128.89, 122.82, 114.27, 114.18, 107.39, 63.10, 55.37, 55.35, 34.20, 26.64		

#### 4.2.5.11. 3-(4-(4-bromophenyl)-6-(4-methoxyphenyl)pyrimidin-2-yl)-2-(4-chlorophenyl)-1,3-thiazinan-4-one (10k)

**Yield,** 25%

**Molecular Weight,** 566.90

**Molecular Formula,** C<sub>27</sub>H<sub>21</sub>BrClN<sub>3</sub>O<sub>2</sub>S



**Procedure:** The intermediate 5 (0.001 mol) was treated with 4-chlorobenzaldehyde (1 eq.), dissolved in 8ml toluene and catalytic amount of glacial acetic acid, as per the procedure given in section 3.2.3.1, to yield desired product **10k**. Column chromatography (Silica gel # 60-120; Hexane:Ethyl acetate : : 80: 20) was performed to afford pure compound.

<b>State &amp; colour:</b>	Light yellow solid	<b>R<sub>f</sub> value:</b>	0.37
----------------------------	--------------------	-----------------------------	------

## CHAPTER 4

## RESULTS AND DISCUSSION

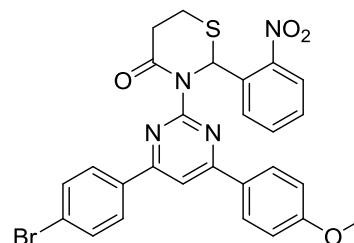
<b>Melting Point:</b>	191-193°C	<b>MS (+ESI) m/z:</b>	568.01 [M+H] <sup>+</sup> , 570.01 [M+2+H] <sup>+</sup>
<b>IR (cm<sup>-1</sup>)</b>	1722 (C=O), 1652 (C=N), 1573 (C=N), 1554 (C=N)		
<b><sup>1</sup>H NMR (400 MHz, CDCl<sub>3</sub>)</b>	8.19 (s, 1H), 7.82-7.79 (m, 4H), 7.60-7.58 (m, 2H), 7.33-7.29 (m, 4H), 6.90-6.88 (2H), 6.45 (s, 1H), 3.04-3.02 (m, 2H), 2.90-2.88 (m, 2H)		
<b><sup>13</sup>C NMR (100 MHz, CDCl<sub>3</sub>)</b>	166.82, 160.17, 160.11, 159.41, 156.93, 136.44, 134.38, 133.97, 131.55, 129.76, 129.58, 129.49, 129.36, 129.28, 122.82, 114.18, 107.39, 62.80, 55.35, 34.20, 26.64		

### 4.2.5.12. 3-(4-(4-bromophenyl)-6-(4-methoxyphenyl)pyrimidin-2-yl)-2-(2-nitrophenyl)-1,3-thiazinan-4-one (10I)

**Yield,** 31%

**Molecular Weight,** 577.45

**Molecular Formula,** C<sub>27</sub>H<sub>21</sub>BrN<sub>4</sub>O<sub>4</sub>S



**Procedure:** The intermediate 5 (0.001 mol) was treated with 2-nitrobenzaldehyde (1 eq.), dissolved in 8ml toluene and catalytic amount of glacial acetic acid, as per the procedure given in section 3.2.3.1, to yield desired product **10I**. Column chromatography (Silica gel # 60-120; Hexane:Ethyl acetate : : 80: 20) was performed to afford pure compound.

**State & colour:** Light yellow solid

**R<sub>f</sub> value:** 0.41

**Melting Point:** 183-185°C

**MS (+ESI) m/z:** 579.04 [M+H]<sup>+</sup>,  
581.04 [M+2+H]<sup>+</sup>

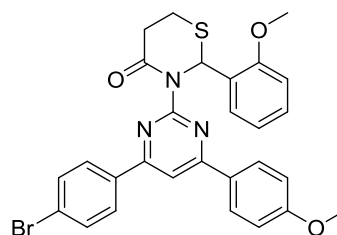
IR (cm <sup>-1</sup> )	1723 (C=O), 1654 (C=N), 1570 (C=N), 1524 (C=N)
<sup>1</sup> H NMR (400 MHz, CDCl <sub>3</sub> )	8.19 (s, 1H), 7.99-7.97 (m, 1H), 7.82-7.79 (m, 4H), 7.72-7.70 (m, 1H), 7.63-7.52 (m, 4H), 7.28 (m, 1H), 6.90-6.88 (m, 2H), 3.80 (s, 3H), 3.07-3.04 (m, 2H), 2.90-2.88 (m, 2H)
<sup>13</sup> C NMR (100 MHz, CDCl <sub>3</sub> )	166.70, 160.17, 160.11, 159.41, 157.14, 147.93, 134.10, 133.97, 132.96, 131.55, 129.76, 129.58, 129.49, 129.44, 128.71, 124.98, 122.82, 114.18, 107.39, 55.74, 55.35, 34.20, 26.55

**4.2.5.13. 3-(4-(4-bromophenyl)-6-(4-methoxyphenyl)pyrimidin-2-yl)-2-(2-methoxyphenyl)-1,3-thiazinan-4-one (10m)**

**Yield,** 29%

**Molecular Weight,** 562.48

**Molecular Formula,** C<sub>28</sub>H<sub>24</sub>BrN<sub>3</sub>O<sub>3</sub>S



**Procedure:** The intermediate 5 (0.001 mol) was treated with 2-methoxybenzaldehyde (1 eq.), dissolved in 8ml toluene and catalytic amount of glacial acetic acid, as per the procedure given in section 3.2.3.1, to yield desired product **10m**. Additionally, column chromatography (Silica gel # 60-120; Hexane:Ethyl acetate : : 80: 20) was performed to afford pure compound.

**State & colour:** Light yellow solid

**R<sub>f</sub> value:** 0.37

**Melting Point:** 183-185°C

**MS (+ESI) m/z:** 563.04 [M+H]<sup>+</sup>,  
565.04 [M+2+H]<sup>+</sup>

IR (cm<sup>-1</sup>) 1723 (C=O), 1654 (C=N), 1570 (C=N), 1524 (C=N)

<sup>1</sup>H NMR (400 MHz, CDCl<sub>3</sub>) 8.19 (s, 1H), 7.99-7.97 (m, 1H), 7.82-7.79 (m, 4H), 7.72-7.70 (m, 1H), 7.63-7.52 (m, 4H), 7.28 (m, 1H), 6.90-6.88 (m, 2H), 3.80 (s, 3H), 3.07-3.04 (m, 2H), 2.90-2.88 (m, 2H)

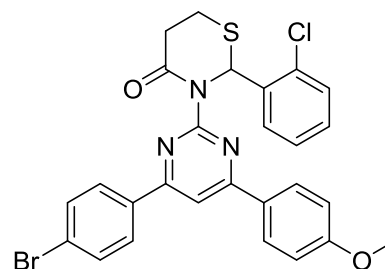
<sup>13</sup>C NMR (100 MHz, CDCl<sub>3</sub>) 166.86, 160.17, 160.11, 159.41, 157.35, 156.94, 133.97, 131.55, 129.76, 129.58, 129.49, 129.40, 128.78, 124.06, 122.82, 122.33, 114.18, 112.75, 107.39, 58.35, 55.62, 55.35, 34.20, 26.62

**4.2.5.14. 3-(4-(4-bromophenyl)-6-(4-methoxyphenyl)pyrimidin-2-yl)-2-(2-chlorophenyl)-1,3-thiazinan-4-one (10n)**

**Yield,** 27%

**Molecular Weight,** 566.90

**Molecular Formula,** C<sub>27</sub>H<sub>21</sub>BrClN<sub>3</sub>O<sub>2</sub>S



**Procedure:** The intermediate 5 (0.001 mol) was treated with 2-chlorobenzaldehyde (1 eq.), dissolved in 8ml toluene and catalytic amount of glacial acetic acid, as per the procedure given in section 3.2.3.1, to yield desired product **10n**. Column chromatography (Silica gel # 60-120; Hexane:Ethyl acetate : : 80: 20) was performed to afford pure compound.

**State & colour:** Light yellow solid

**R<sub>f</sub> value:** 0.37

**Melting Point:** 194-196°C

**MS (+ESI) m/z:** 568.04 [M+H]<sup>+</sup>,  
570.04 [M+2+H]<sup>+</sup>

**IR (cm<sup>-1</sup>)** 1723 (C=O), 1654 (C=N), 1570 (C=N), 1524 (C=N)

<sup>1</sup>H NMR (400 MHz, CDCl<sub>3</sub>) 8.19 (s, 1H), 7.82-7.79 (m, 4H), 7.60-7.58 (m, 2H), 7.45-



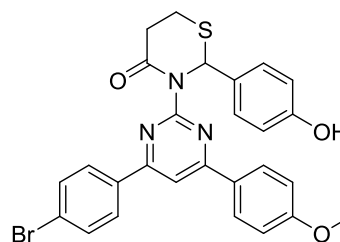
CDCl <sub>3</sub> )	7.27 (m, 4H), 6.90-6.86 (m, 3H), 3.80 (s, 3H), 3.07-3.05 (m, 2H), 2.90-2.88 (m, 2H)
<sup>13</sup> C NMR (100 MHz, CDCl <sub>3</sub> )	166.83, 160.17, 160.11, 159.41, 156.68, 135.96, 133.97, 132.94, 131.55, 130.33, 129.90, 129.76, 129.70, 129.58, 129.49, 128.04, 122.82, 114.18, 107.39, 57.94, 55.35, 34.20, 26.65

**4.2.5.15. 3-(4-(4-bromophenyl)-6-(4-methoxyphenyl)pyrimidin-2-yl)-2-(4-hydroxyphenyl)-1,3-thiazinan-4-one (10o)**

**Yield, 36%**

**Molecular Weight, 548.46**

**Molecular Formula, C<sub>27</sub>H<sub>22</sub>BrN<sub>3</sub>O<sub>3</sub>S**



**Procedure:** The intermediate 5 (0.001 mol) was treated with 4-hydroxybenzaldehyde (1 eq.), dissolved in 8ml toluene and catalytic amount of glacial acetic acid, as per the procedure given in section 3.2.3.1, to yield desired product **10o**. Additionally, column chromatography (Silica gel # 60-120; Hexane:Ethyl acetate : : 80: 20) was performed to afford pure compound.

**State & colour:** Light yellow solid

**R<sub>f</sub> value:** 0.38

**Melting Point:** 187-189°C

**MS (+ESI) m/z:** 549.04 [M+H]<sup>+</sup>,  
551.04 [M+2+H]<sup>+</sup>

**IR (cm<sup>-1</sup>)** 1723 (C=O), 1654 (C=N), 1570 (C=N), 1524 (C=N)

**<sup>1</sup>H NMR (400 MHz,** 8.19-8.16 (m, 2H), 7.82-7.79 (m, 4H), 7.60-7.58 (m, 2H),

**CDCl<sub>3</sub>)** 7.19-7.17 (m, 2H), 6.90-6.88 (m, 2H), 6.80-6.78 (m, 2H),  
6.44 (s, 1H), 3.80 (s, 3H), 3.04-3.02 (m, 2H), 2.90-2.88

---

	(m, 2H)
<sup>13</sup> C NMR (100 MHz, CDCl <sub>3</sub> )	166.82, 160.17, 160.11, 159.41, 157.92, 156.93, 133.97, 131.55, 130.08, 129.76, 129.58, 129.55, 129.49, 122.82, 116.09, 114.18, 107.39, 63.22, 55.35, 34.20, 26.64

### 4.3. BIOLOGICAL EVALUATION

#### 4.3.1. Enzymatic activity

The ERK2 inhibitory potential of all the 30 synthesized compounds belonging to Formula I and II was determined by *in vitro* enzymatic assay. Ulixertinib, used for screening the lead molecule in our *in-silico* study, was selected as standard in the assay, accordingly required controls (C<sub>100%</sub>, C<sub>0%</sub>, F<sub>100%</sub> and F<sub>0%</sub>) and test samples (conc. of synthesized compounds) were used. Following the estimation of predicted activity, three concentration points, 0.1, 1 and 10 μM, were taken for the test compounds and IC<sub>50</sub> values were determined to characterize the inhibitory potential. Except for one or two outliers, in general the compounds predicted to bind well as per the MM-GBSA analysis and showed good potency in the biochemical assay. From compounds belonging to Formula I, Compound **8j**, with best binding affinity score in MM-GBSA analysis, with a –OCH<sub>3</sub> substitution at the para position of the aryl ring coupled with the thiazolidinone nucleus and methoxy-aryl ring substituted on the pyrimidine ring showed best inhibitory activity with IC<sub>50</sub> = 0.347μM. Another compound **8c**, IC<sub>50</sub> = 0.512μM, having a methoxy substituent at the ortho position of thiazolidinone coupled aryl ring was also found to be a modest ERK2 inhibitor. Interestingly, this molecule was derived from the bromo substituted bi-aryl pyrimidine system, which clearly suggests that orientation imparted due to the bi-aryl pyrimidine system is more correlated to the activity than the specific substituent on the 2-phenyl ring of thiazolidin-4-one nucleus. However, substituting second methoxy group, **8e** and **8f**, on the same ring did not improve the activity, which fell to IC<sub>50</sub> =

0.781 $\mu$ M and 1.223 $\mu$ M, respectively, validating the *in-silico* results which suggested that bulky molecules had altered binding mode and interacted poorly with the catalytic domain residues. Expectedly, the molecule, **8h**, having an unsubstituted aryl ring coupled to the thiazolidinone nucleus was found to be one of the less potent molecules amongst the pool with  $IC_{50} = 1.151\mu$ M. The detailed result of enzymatic activity is summarized in **Table 4.17**.

**Table 4.17.** ERK2 inhibitory potential of the compounds (**8a-8o**) as per the *in-vitro* enzymatic assay.

S.No.	Compound ID	R	R <sub>1</sub>	R <sub>2</sub>	IC <sub>50</sub> ( $\mu$ M)
1.	8a	4-Cl	Br	Cl	2.605
2.	8b	2-Cl	Br	Cl	0.683
3.	8c	2-OCH <sub>3</sub>	Br	Cl	0.512
4.	8d	4-OH	Br	Cl	0.954
5.	8e	2,5-di-OCH <sub>3</sub>	Br	Cl	0.781
6.	8f	2,4-di-OCH <sub>3</sub>	Br	Cl	1.223
7.	8g	4-NO <sub>2</sub>	Br	Cl	0.961
8.	8h	H	Br	Cl	1.151
9.	8i	2-NO <sub>2</sub>	Br	Cl	0.881
10.	<b>8j</b>	<b>4-OCH<sub>3</sub></b>	<b>Br</b>	<b>OCH<sub>3</sub></b>	<b>0.347</b>
11.	8k	4-Cl	Br	OCH <sub>3</sub>	0.602
12.	8l	2-NO <sub>2</sub>	Br	OCH <sub>3</sub>	0.692
13.	8m	2-OCH <sub>3</sub>	Br	OCH <sub>3</sub>	0.872
14.	8n	2-Cl	Br	OCH <sub>3</sub>	1.035
15.	8o	4-OH	Br	OCH <sub>3</sub>	0.791
16.	Ulixertinib	-----	-----	-----	0.012

From compounds belonging to formula II, compound **10h** bearing unsubstituted phenyl ring on 1,3-thiazinan-4-one nucleus having the highest binding affinity score (MM-GBSA score) amongst all compounds, also showed best inhibitory activity against ERK2 with IC<sub>50</sub> value of 0.103 μM (Table 4.18.). It has been observed that compounds with methoxy substituent at the para position of 1,3-thiazinan-4-one coupled aryl ring were found to exhibit less inhibitory ERK2 inhibitory activity. Results indicated that although increasing the ring size did improve the binding pocket occupancy but it also altered the binding conformation and hampered the previous protein-ligand interactions when compared to five-membered series compounds. The observed inhibitory potential for the compounds can be, not explicitly, generalized and understood well by the MM-GBSA score which in this case is dependent on the hydrophobic interactions between binding pocket residues and substituted aryl ring coupled to the 1,3-thiazinan-4-one nucleus.

**Table 4.18.** *In-vitro* ERK2 inhibitory data of the designed compounds (**10a-10o**).

S.No.	Compound ID	R	R <sub>1</sub>	R <sub>2</sub>	IC <sub>50</sub> (μM)
1.	10a	4-Cl	Br	Cl	0.514
2.	10b	2-Cl	Br	Cl	0.587
3.	10c	2-OCH <sub>3</sub>	Br	Cl	0.615
4.	10d	4-OH	Br	Cl	0.285
5.	10e	2,5-di-OCH <sub>3</sub>	Br	Cl	0.540
6.	10f	2,4-di-OCH <sub>3</sub>	Br	Cl	0.396
7.	10g	4-NO <sub>2</sub>	Br	Cl	0.187
8.	<b>10h</b>	<b>H</b>	<b>Br</b>	<b>Cl</b>	<b>0.103</b>
9.	10i	2-NO <sub>2</sub>	Br	Cl	0.497
10.	10j	4-OCH <sub>3</sub>	Br	OCH <sub>3</sub>	0.768
11.	10k	4-Cl	Br	OCH <sub>3</sub>	0.897

12.	10l	2-NO <sub>2</sub>	Br	OCH <sub>3</sub>	0.713
13.	10m	2-OCH <sub>3</sub>	Br	OCH <sub>3</sub>	0.523
14.	10n	2-Cl	Br	OCH <sub>3</sub>	0.682
15.	10o	4-OH	Br	OCH <sub>3</sub>	0.718
16.	Ulixertinib	-----	-----	-----	0.012

### 4.3.2. Anti-cancer activity

Finally, evaluation of the anti-proliferative potential of the most potent ten compounds from both Formula I and II, as per enzymatic assay, was done by performing MTT assay against breast cancer cell lines (MCF7 and MDA-MB-231) and lung cancer cell line (A549) showing expression of MAPK pathway (Lau, Chen et al. 2009). IC<sub>50</sub> value corresponding to each compound, given in the **Table 4.19**, represent the median effect dose (in  $\mu\text{M}$ ) at which 50% cells are inhibited.

In the MTT assay, against MCF7 cell line, compounds **8j**, **8l**, **8k**, **8c** and **10i** showed commendable inhibitory potential. Out of the pool, **8j** showed significant anti-proliferative potential with 85.42%, 64.48%, 42.76% and 30.66% cell viability at 10 $\mu\text{M}$ , 20 $\mu\text{M}$ , 30 $\mu\text{M}$  and 40 $\mu\text{M}$  concentration, respectively. Compound **8j** was followed by **8k**, which also showed commendable anti-proliferative potential with 72.72%, 53.73%, 39.77% and 21.68% cell viability at 10 $\mu\text{M}$ , 20 $\mu\text{M}$ , 30 $\mu\text{M}$  and 40 $\mu\text{M}$  concentration, respectively (**Figure 4.16**). The anti-proliferative potential of the tested compound followed the typical pattern observed in the biochemical assay. An interesting outlier was NO<sub>2</sub> containing compound, **8l** showing an improved cytotoxic potential which can be accredited to its well-known toxicophoric profile. However, the potency of all the compounds was 30-40 times lower in the cellular assay, which can be attributed to the fact that molecules need to penetrate through cell membrane which in turn is influenced by the pharmacokinetic profile of the molecules. Overall, strong hydrophobic interaction which in turn improved the binding can be considered as the reason for best activity profile of **8j** with IC<sub>50</sub> = 18.51 $\mu\text{M}$ . Similarly, other compounds with methoxy substitution on R<sub>2</sub>, compound **8k** and **8l**, also showed

potent anti-proliferative potential with the  $IC_{50} = 20.09\mu\text{M}$  and  $19.29\mu\text{M}$ , respectively. **Figure 4.16.** presents the obtained results as graph plotted between % viability (Mean  $\pm$  S.D.) and concentrations of the test compounds (**8b**, **8c**, **8j**, **8k** and **8l**).

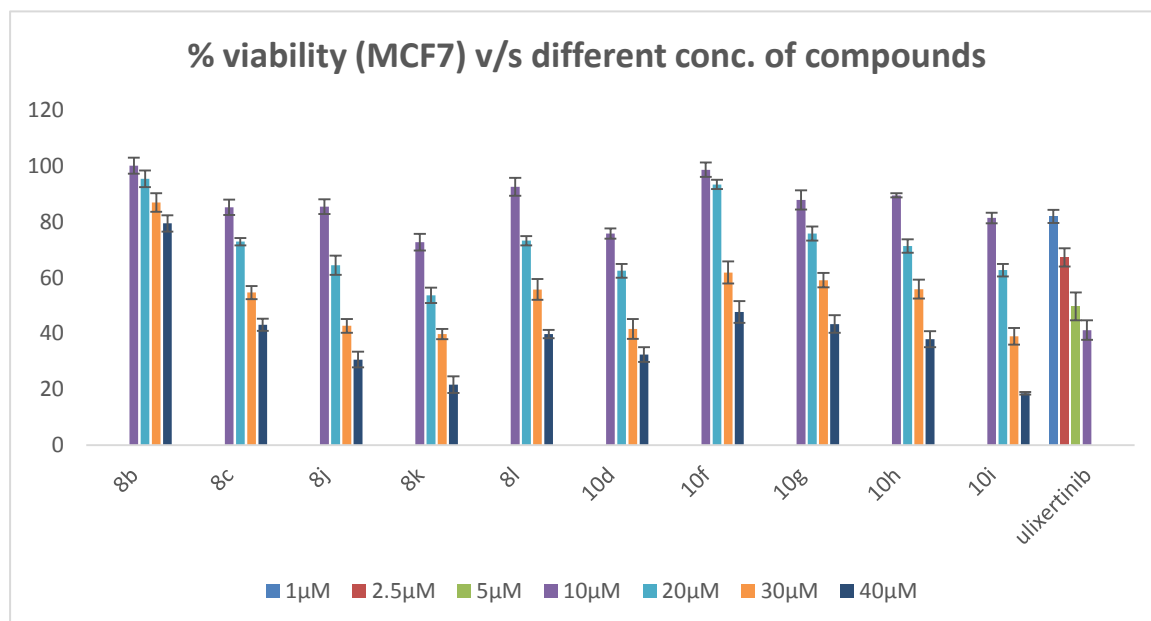


**Figure 4.16.** Percent viability vs concentration plot of MCF7 in response to treatment with synthesized compounds after 48 h. Data is expressed as mean values  $\pm$  S.D. of three independent experiments.

Against A549 cell line, compounds **8k** and **10i** showed commendable inhibitory potential (**Table 4.19.**). Out of the pool, **8k** showed significant anti-proliferative potential with 89.65%, 79.64%, 65.27%, and 43.36% cell viability at 10µM, 20µM, 30µM and 40µM concentration, respectively. Compound **8k** was followed by **10i**, which also showed commendable anti-proliferative potential with 86.31%, 74.95%, 57.18%, and 43.82% cell viability at 10µM, 20µM, 30µM and 40µM concentration, respectively (**Figure 4.17.**). Rest of the compounds did not show significant anti-proliferative potential against A549 cell line and one explanation could be independence of these cells from MAPK pathway for growth and survival, while the

other reason could be failure of the compounds to permeate through the cell membrane to show its action.

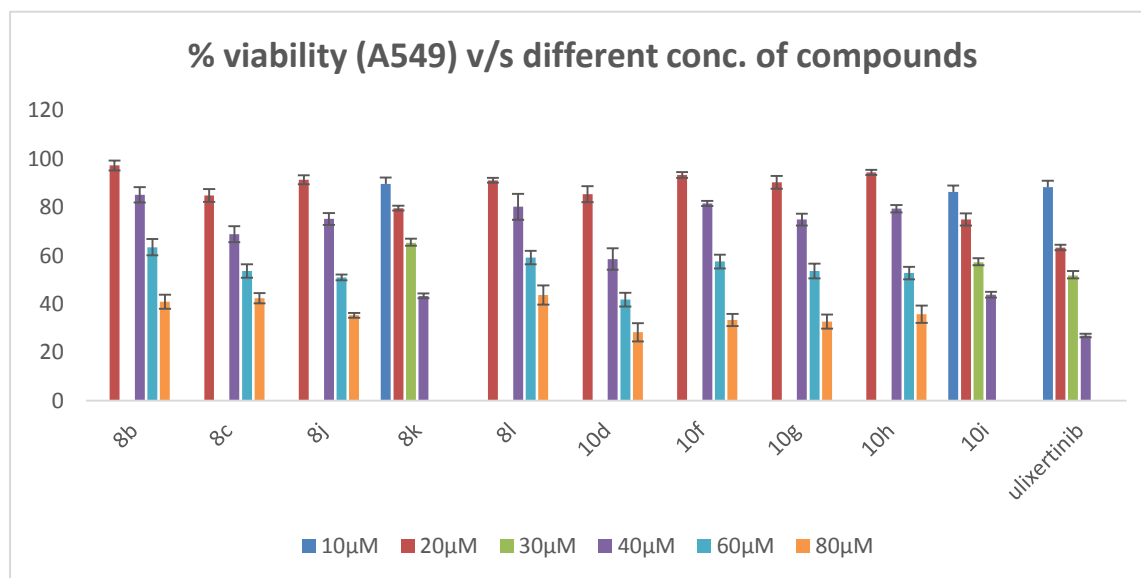


**Figure 4.17.** Percent viability vs concentration plot of A549 in response to treatment with synthesized compounds after 48 h. Data is expressed as mean values  $\pm$  S.D. of three independent experiments.

Against MDA-MB-231 cell line, compounds **10d**, **10f**, **10i**, **8j**, and **8c** showed significant inhibitory potential. Out of the pool, **10d** showed significant anti-proliferative potential with 88.56%, 65.44%, 40.70%, and 20.29% cell viability at 10µM, 20µM, 30µM and 40µM concentration, respectively. Compound **10d** was followed by **10f**, which also showed commendable anti-proliferative potential with 95.63%, 81.67%, 65.41%, and 40.79% cell viability at 10µM, 20µM, 30µM and 40µM concentration, respectively (**Figure 4.18.**). One key fact observed during the evaluation of anti-proliferative potential against MDA-MB-231 was that the compounds belonging to Formula II i.e., compounds with increased ring size fared better than compounds pertaining to Formula I. These results also validated the *in-silico* observation that upon increasing ring size the ligand packing improved,

resulting in better binding affinity (also observed in MM-GBSA). One reason for the improved activity could be the fact that MDA-MB-231 cell line represents TNBC, which does not express usual molecular target, but relies mainly on signaling pathways such as MAPK for growth and survival. Overall, improved fit value which in turn improved the binding can be considered as the reason for best activity profile of **10d** with  $IC_{50} = 21.78\mu M$ . Similarly, compound **10f** and **10i**, also showed potent anti-proliferative potential with the  $IC_{50} = 27.65\mu M$  and  $24.80\mu M$ , respectively.

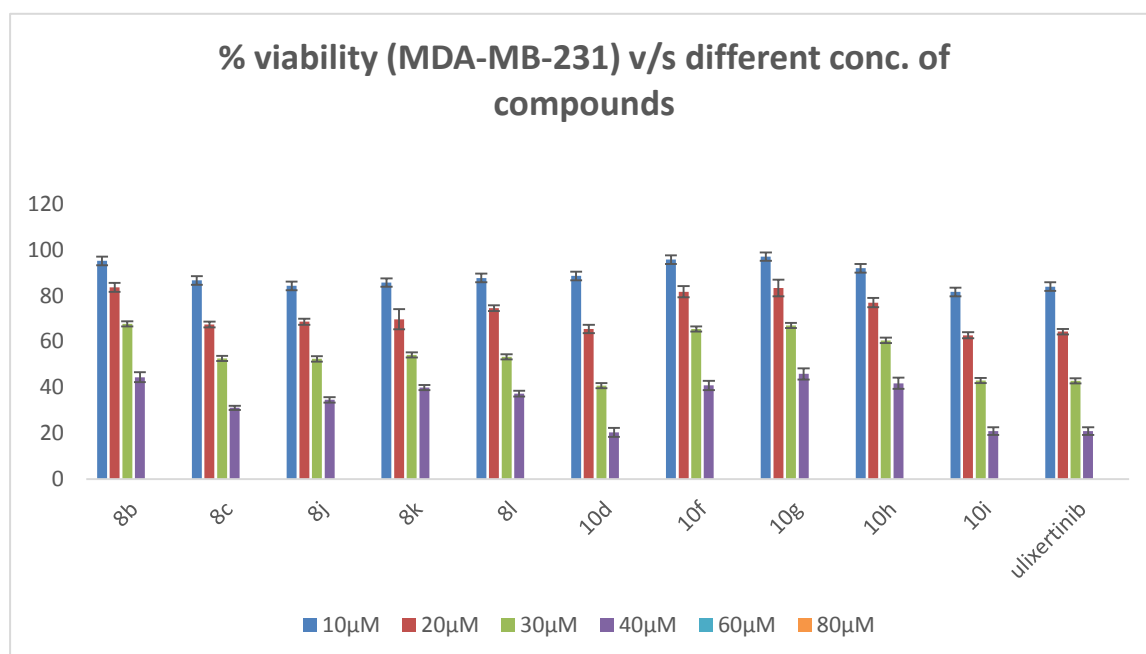


**Figure 4.18.** Percent viability vs concentration plot of MDA-MB-231 in response to treatment with synthesized compounds after 48 h. Data is expressed as mean values  $\pm$  S.D. of three independent experiments.

**Table 4.19.** *In-vitro* anti-proliferative data of the top compounds against different cell lines (MCF7, A549 and MDA-MB-231).

S.No.	Compound ID	MCF7 ( $\mu M \pm SD$ )*	A549 ( $\mu M \pm SD$ )*	MDA-MB-231 ( $\mu M \pm SD$ )*
1.	8b	47.21 ( $\pm 3.01$ )	52.45 ( $\pm 2.90$ )	29.74 ( $\pm 1.85$ )



2.	8c	23.47 ( $\pm$ 2.14)	70.05 ( $\pm$ 3.61)	27.54 ( $\pm$ 2.33)
3.	8j	18.51 ( $\pm$ 2.84)	51.97 ( $\pm$ 2.69)	30.24 ( $\pm$ 1.13)
4.	8k	20.09 ( $\pm$ 2.64)	32.63 ( $\pm$ 2.44)	32.65 ( $\pm$ 1.20)
5.	8l	19.29 ( $\pm$ 2.54)	61.19 ( $\pm$ 1.05)	29.00 ( $\pm$ 2.22)
6.	10d	33.13 ( $\pm$ 2.64)	53.10 ( $\pm$ 2.03)	21.78 ( $\pm$ 1.25)
7.	10f	27.10 ( $\pm$ 3.02)	49.01 ( $\pm$ 2.22)	27.65 ( $\pm$ 2.22)
8.	10g	33.17 ( $\pm$ 2.92)	51.52 ( $\pm$ 2.60)	29.46 ( $\pm$ 2.86)
9.	10h	29.41 ( $\pm$ 2.34)	49.30 ( $\pm$ 2.12)	29.94 ( $\pm$ 2.07)
10.	10i	23.56 ( $\pm$ 1.88)	34.43 ( $\pm$ 1.89)	24.80 ( $\pm$ 1.51)
11.	Ulixertinib	9.14 ( $\pm$ 3.52)	25.57 ( $\pm$ 1.24)	23.76 ( $\pm$ 1.31)

\* the values represent IC<sub>50</sub> values, expressed as median effect dose in  $\mu$ M at which 50% cells are inhibited

### 4.3.3. Normal cell toxicity

Furthermore, top compounds were tested against normal breast cells using HBL-100 cell line to evaluate their toxicity. All the compounds were found to be non-toxic at 40 $\mu$ M. Compounds belonging to Formula II were also non-toxic at 80 $\mu$ M, while compounds belonging to Formula I showed mild toxicity at 80 $\mu$ M. Overall in the results, compounds 10d, 10f, 10g, 10h and 8b showed more than 90% cell viability for normal breast cells (HBL-100 cell line) until 40 $\mu$ M. **Figure 4.19.** presents the obtained results as graph plotted between % viability (Mean  $\pm$  S.D.) and concentrations of the test compounds.

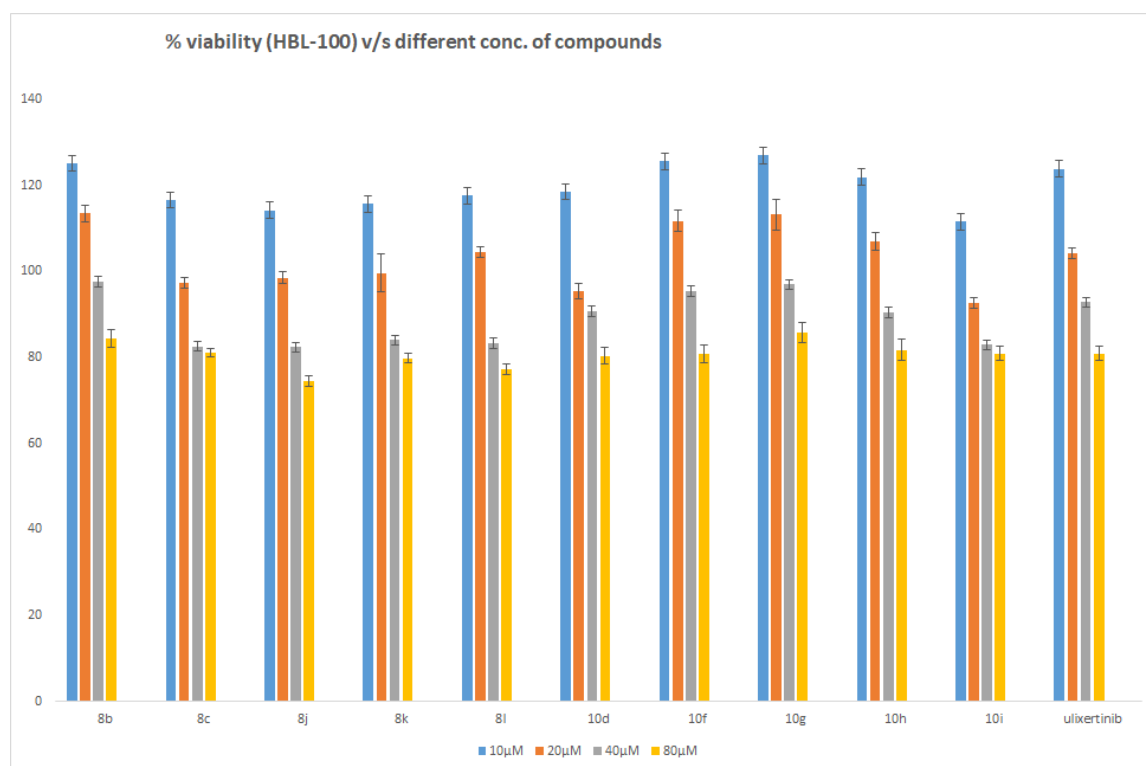


**Figure 4.19.** Percent viability vs concentration plot of HBL-100 in response to treatment with synthesized compounds after 48 h. Data is expressed as mean values  $\pm$  S.D. of three independent experiments.

#### 4.4. STRUCTURAL ACTIVITY RELATIONSHIP (SAR) STUDY

From the biological study and *in-silico* study, some key structural features are observed for the compounds pertaining to Formula I which are responsible for good ERK2 inhibitory activity. These are discussed as below:

##### 4.4.1. For Formula I compounds (thiazolidinone-pyrimidine derivatives)

1. Introduction of methoxy group at the para position of the aryl side chain coupled with the thiazolidinone nucleus and methoxy-aryl ring substituted on

the pyrimidine ring was observed to be important for activity (Compound 8j with  $IC_{50} = 0.347 \mu\text{M}$ ).

2. Presence of methoxy substituent at the ortho position of thiazolidinone coupled aryl ring, was also found to showed modest ERK2 inhibitory activity (compound 8c with  $IC_{50} = 0.512 \mu\text{M}$ ).
3. Orientation imparted due to the bi-aryl pyrimidine system is more correlated to the activity than the specific substituent on the 2-phenyl ring of thiazolidin-4-one nucleus.
4. Substitution of bulky group like di- methoxy group, on the same ring exhibit less ERK2 inhibitory activity (Compound 8e and 8f with  $IC_{50} = 0.781 \mu\text{M}$  and  $1.223 \mu\text{M}$ , respectively), validating the *in-silico* results which suggested that bulky molecules had altered binding mode and interacted poorly with the catalytic domain residues.
5. Unsubstituted aryl ring coupled to the thiazolidinone nucleus was found to be one of the less potent molecules, thus highlights the significance of substituents on 2-phenyl ring of thiazolidin-4-one nucleus. The graphical representation of the SAR of the thiazolidinone-pyrimidine derivatives for the ERK2 inhibitory activity has been shown in **Figure 4.20**.

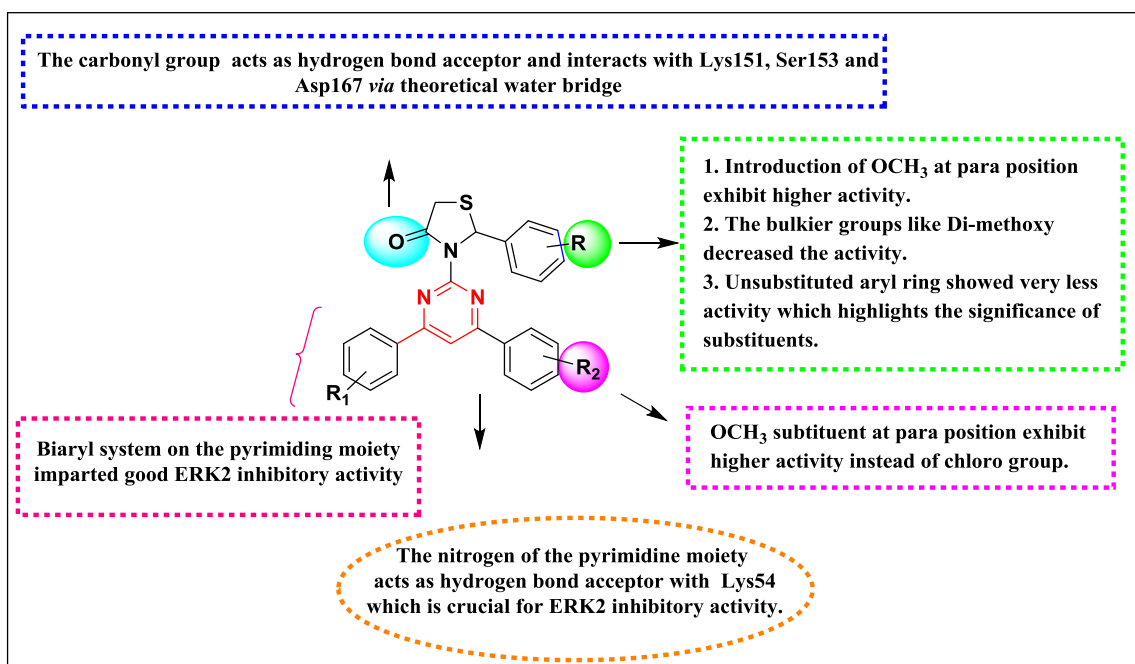


**Figure 4.20.** SAR of the thiazolidinone-pyrimidine derivatives for the ERK2 inhibitory activity.

#### 4.4.2. For Formula II compounds (thiazinanone-pyrimidine derivatives)

1. Changing thiazolidinone to thiazinanone altered the binding pattern in the protein activity and thus exhibit MMGBSA score differently for each derivative when compared to five-membered derivatives.
2. Also, the substitution pattern on aryl ring coupled with thiazinanone nucleus showed change in the ERK2 inhibitory activity in comparison to five-membered derivatives.
3. Substitution of bulky groups at R position on aryl ring exhibited less ERK2 inhibitory activity.

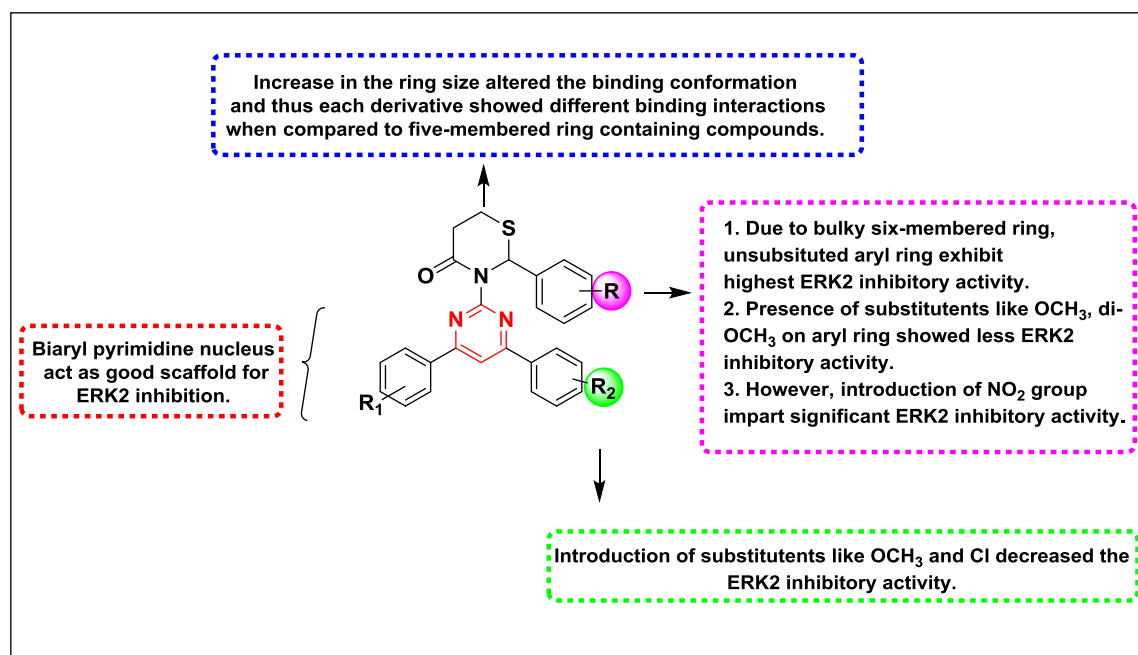


**Figure 4.21.** SAR of the thiazinanone-pyrimidine derivatives for the ERK2 inhibitory activity.

4. While derivative having aryl ring with no substitution (compound 10h with  $IC_{50} = 0.103 \mu M$ ) exhibited highest ERK2 inhibitory activity among all the synthesized derivatives. The graphical representation of the SAR of the thiazinanone-pyrimidine derivatives for the ERK2 inhibitory activity has been shown in **Figure 4.21**.